



EEE598 – Renewable Electric Energy Systems

DFIG Converter Control for Wind Turbine

Name: Ahmed Fahmy

Table of Contents

EEE598 – Renewable Electric Energy Systems	1
DFIG Converter Control for Wind Turbine	1
Table of figures	3
Introduction	5
Specifications	5
Part A.....	5
Part B.....	11
Part C.....	27
Control design parameters	33
Appendix	33
Appendix A.....	33

Table of figures

Figure 1 DFIG PLECS Model.....	6
Figure 2 Electromagnetic torque in Nm (above curve) and rotor mechanical speed in rad/sec.....	7
Figure 3 Stator and rotor currents in dq reference frame.....	7
Figure 4 Stator currents in abc reference frame.....	8
Figure 5 Rotor Current in abc reference frame	8
Figure 6 DFIG equivalent circuit.....	9
Figure 7 Turbine model in PLECS	11
Figure 8 Active and Reactive power control block diagram	12
Figure 9 Active and reactive power control in PLECS	13
Figure 10 Rotor current control block diagram	14
Figure 11 Rotor current control PLECS model	14
Figure 12 Mechanical speeds at for wind speeds	15
Figure 13 Mechanical Power from MPPT and grid injected power for different wind speeds	15
Figure 14 rotor d-axis current for different wind speeds	16
Figure 15 rotor q-axis current for different wind speeds	16
Figure 16 abc rotor current for wind speed 12 m/sec.....	17
Figure 17 abc rotor current for wind speed 12 m/sec.....	17
Figure 18 stator q-axis current for different wind speeds.....	18
Figure 19 stator d-axis current for different wind speeds.....	18
Figure 20 Stator abc current at wind speed 12 m/sec.....	18
Figure 21 stator abc current at wind speed 8 m/sec	19
Figure 22 Stator abc voltages for different wind speeds.....	19
Figure 23 Stator dq voltages for different wind speeds	20
Figure 24 Rotor abc voltages for different wind speeds.....	20
Figure 25 Rotor dq voltages for different wind speeds	20
Figure 26 Mechanical speed reference and measured.....	22
Figure 27 Mechanical power and power grid injected power.....	23
Figure 28 Rotor dq-axis voltages.....	23
Figure 29 Rotor abc reference frame voltages	24
Figure 30 Rotor side dq-axis currents	24
Figure 31 Stator abc reference frame currents	25
Figure 32 Rotor dq-axis currents.....	25
Figure 33 abc reference frame rotor currents	26
Figure 34 RSC and GSC models in PLECS.....	27
Figure 35 GSC Current control block diagram.....	27
Figure 36 DC link voltage control block diagram	28
Figure 37 DC link voltage control in PLECS	28
Figure 38 GSC current control in PLECS	29
Figure 39 Over all block diagram of the system.....	29
Figure 40 Stator abc current at wind speed 12 m/sec.....	30
Figure 41 Stator abc current at wind speed 9 m/sec.....	30

Figure 42 Rotor side abc currents at wind speeds 12 and 9 m/sec	30
Figure 43 Rotor side abc voltages at wind speed 12 m/sec and 9 m/sec.....	31
Figure 44 Vdc link at wind speed 9 m/sec	31
Figure 45 Rotor mechanical speed at wind speed 9 m/sec	32
Figure 46 GSC voltage in abc axis at wind speed 9 m/sec	32
Figure 47 GSC current in abc frame at wind speed 9 m/sec.....	32

Introduction

This document discusses modeling, steady state and dynamic analysis, controller design and simulation of a DFIG based wind generator. The document consists of three parts A, B, C. Part A discusses the modelling of the DFIG as a squirrel cage machine, and rotor is short-circuited to study the steady state and dynamic analysis of the machine. Part B discusses the RSC (Rotor Side Converter) control and how to control the active and reactive power as well as the MPPT to extract the maximum possible power from the turbine. Averaged block diagram models are used for part A and B. Part C discusses GSC (Grid Side Converter) and the control of the DC link. In this part switched model is integrated with the above models.

Specifications

The machine used for simulation is a 1.5 MW DFIG machine with the below parameters.

R_s (Ω)	R_r (Ω)	L_{ls} (mH)	L_{lr} (mH)	L_m (mH)	P	C_{dc} (F)	B (Nm/(rad/sec))	J (Kg.m ²)	S_{rated} (MW)
0.0046	0.0032	0.0947	0.0842	1.526	6	0.005	1e-3	100	1.37

$$V_{dc} = 1150V$$

$$V_{grid\ L-L} = 575V$$

$$f_{grid} = 60\text{hz}$$

Part A

In this part, The DFIG modeled as squirrel cage motor so $V_r = 0$ based on the below equations and the model is presented below in figure1.

$$\begin{aligned} \frac{d}{dt} \begin{bmatrix} \lambda_{sd} \\ \lambda_{sq} \end{bmatrix} &= \begin{bmatrix} v_{sd} \\ v_{sq} \end{bmatrix} - R_s \begin{bmatrix} i_{sd} \\ i_{sq} \end{bmatrix} - \omega_d * M_{rotate} * \begin{bmatrix} \lambda_{sd} \\ \lambda_{sq} \end{bmatrix} \\ \frac{d}{dt} \begin{bmatrix} \lambda_{rd} \\ \lambda_{rq} \end{bmatrix} &= \begin{bmatrix} v_{rd} \\ v_{rq} \end{bmatrix} - R_s \begin{bmatrix} i_{rd} \\ i_{rq} \end{bmatrix} - \omega_{dA} * M_{rotate} * \begin{bmatrix} \lambda_{rd} \\ \lambda_{rq} \end{bmatrix} \end{aligned}$$

$$\begin{bmatrix} \lambda_{sd} \\ \lambda_{sq} \\ \lambda_{rd} \\ \lambda_{rq} \end{bmatrix} = M \begin{bmatrix} i_{sd} \\ i_{sq} \\ i_{rd} \\ i_{rq} \end{bmatrix}$$

$$T_{em} = \frac{P}{2} L_m (i_{sq} i_{rd} - i_{sd} i_{rq})$$

$$\frac{d}{dt} \omega_{mech} = \frac{T_{em} - T_L}{J_{eq}}$$

Where

$$M = \begin{bmatrix} L_s & 0 & L_m & 0 \\ 0 & L_s & 0 & L_m \\ L_m & 0 & L_r & 0 \\ 0 & L_m & 0 & L_r \end{bmatrix}$$

And

$$M_{rotate} = \begin{bmatrix} 0 & -1 \\ 1 & 0 \end{bmatrix}$$

In figure 1 the currents are calculated from the flux linkages through gain K which is the inverse matrix of M. The inverse matrix is calculated through the simple MATLAB script in appendix A.

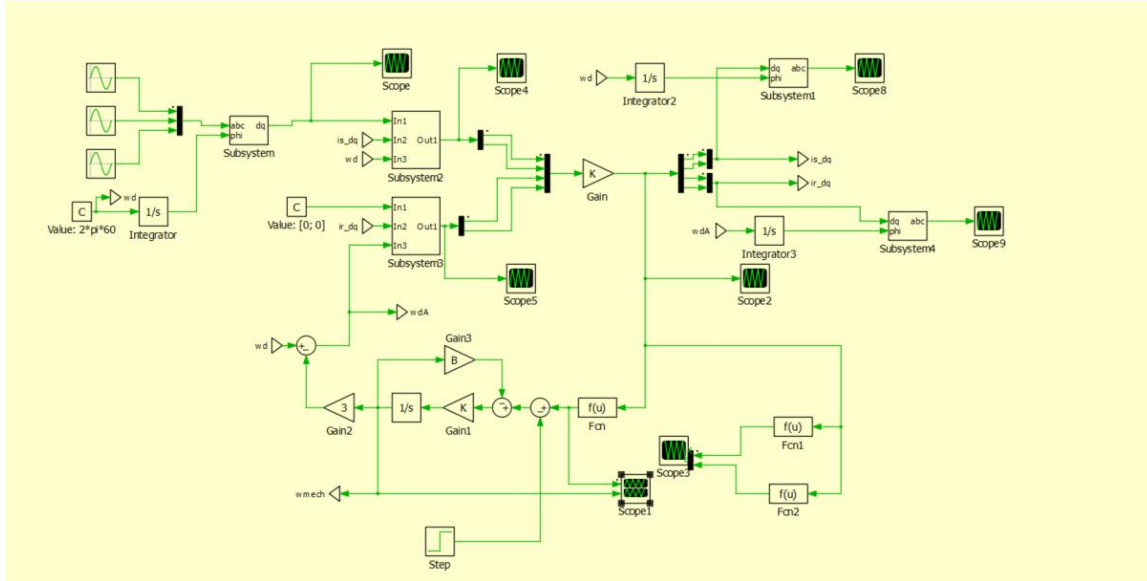


Figure 1 DFIG PLECS Model

The load torque is modeled for this part as a step of initial value 5000Nm (motoring mode) then changes to -5000Nm (generator mode) and the below figures show the results of the simulation

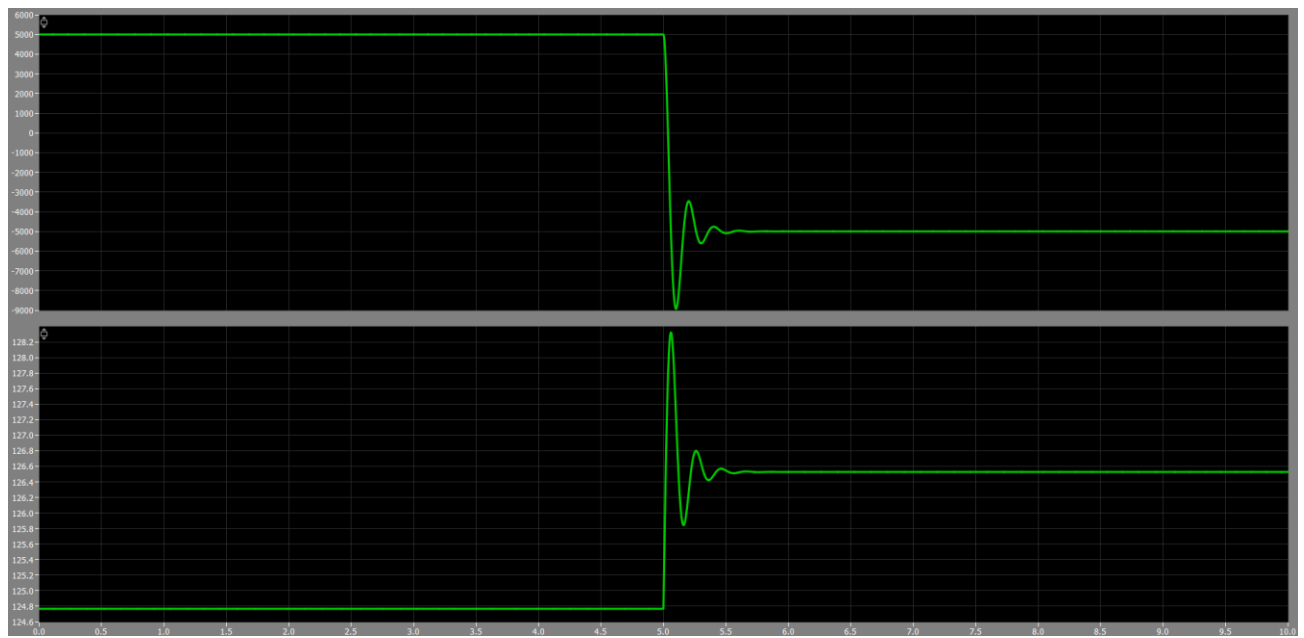


Figure 2 Electromagnetic torque in Nm (above curve) and rotor mechanical speed in rad/sec



Figure 3 Stator and rotor currents in dq reference frame

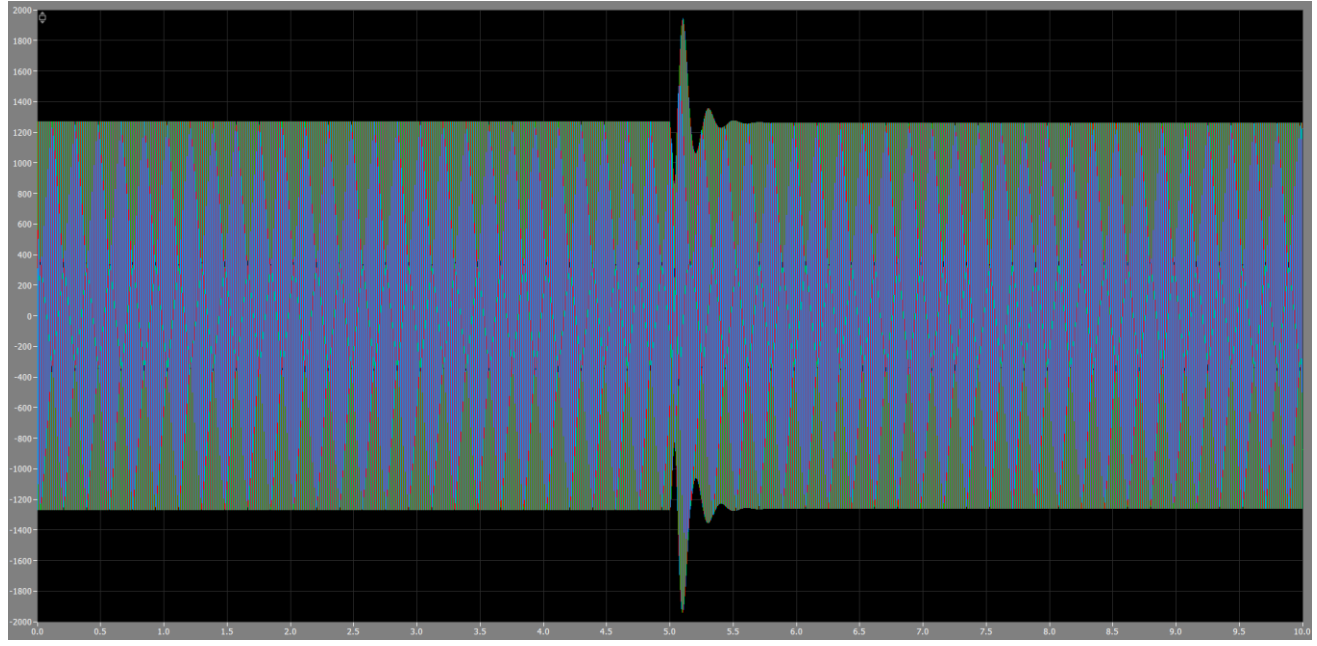


Figure 4 Stator currents in abc reference frame

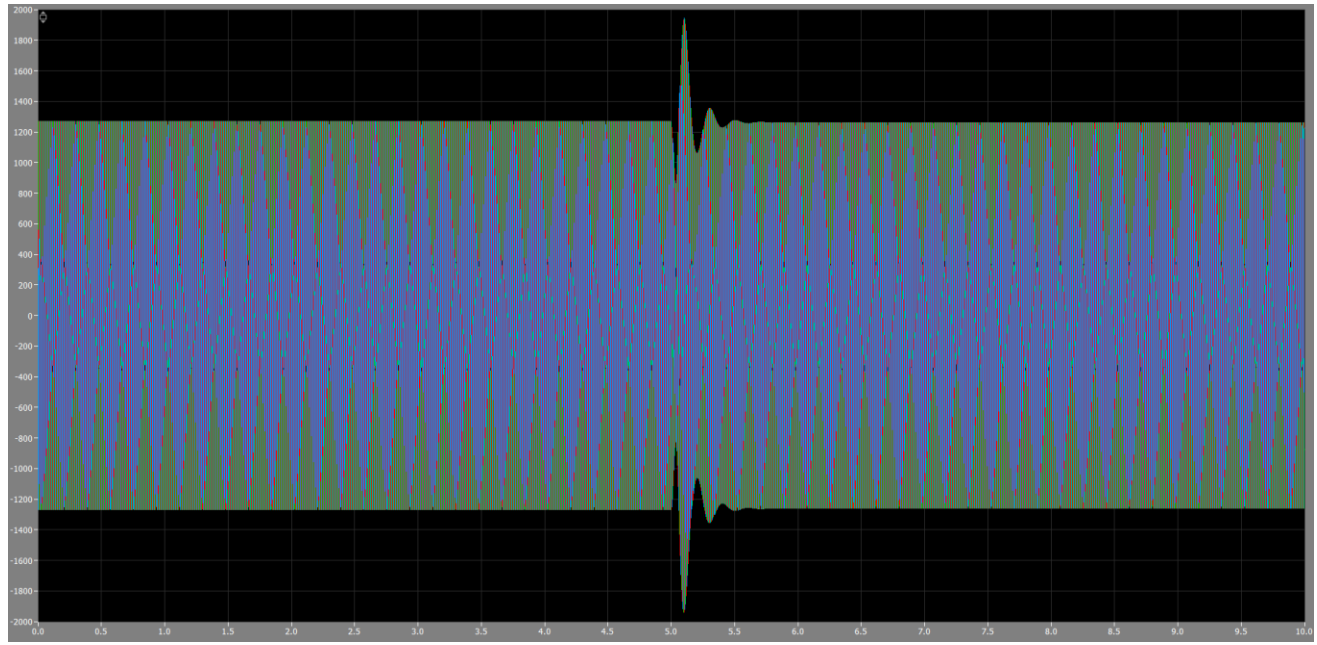


Figure 5 Rotor Current in abc reference frame

As shown in figure 2, $T_{em} = T_L = 5000$ for the first part of the simulation which is expected to avoid any acceleration in the steady state and the mechanical speed is 124.77 rad/sec while the synchronous speed is $120*f/p = 125.664$ rad/sec which means that the slip is $s = 7.133 \times 10^{-3}$ using the below equation

$$S = \frac{\omega_{synch} - \omega_r}{\omega_{synch}}$$

By solving analytically, we get:

$$\omega_{mech} = \omega_{synch} * (1 - s) = 124.77 \text{ rad/sec} \quad \& \quad T_{em} = T_L = 5000 \text{ Nm}$$

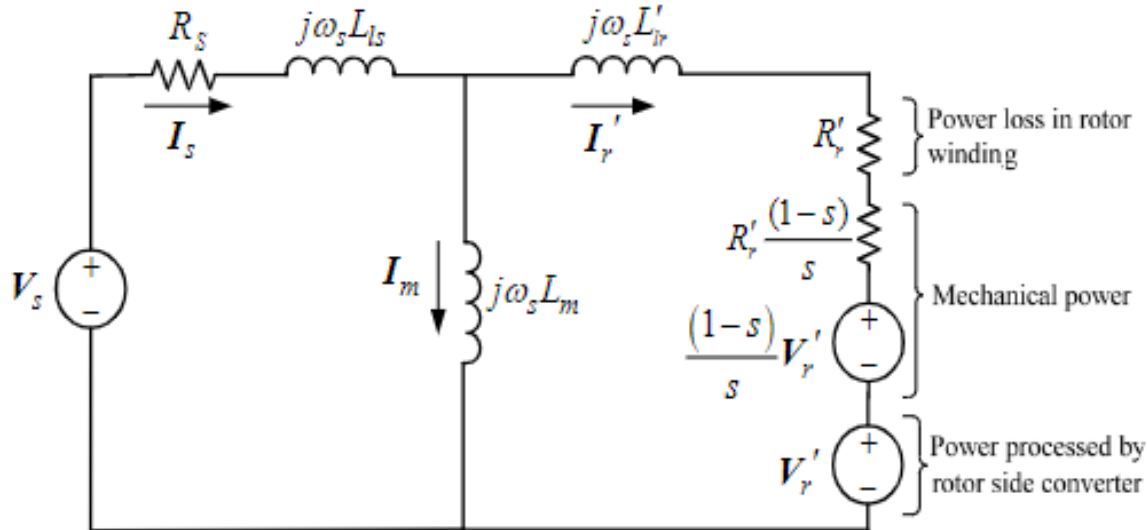


Figure 6 DFIG equivalent circuit

By solving the circuit in figure 6 analytically where

$$V_s = \frac{575}{\sqrt{3}} \text{ V} \quad \& \quad V_r = 0 \text{ V}$$

$$I_s = \frac{V_s}{(R_s + j\omega_s L_{ls}) + (j\omega_s L_m) // (j\omega_s L_{lr} + \frac{R'_r}{s})} = 644.98 - j622.85 \text{ A}$$

$$I_{s,dq} = \frac{3\sqrt{2}}{2} I_s = 1368.21 - j1321.27$$

$$i_{sd} = \sqrt{\frac{2}{3}} \operatorname{Re}[I_{s,dq}] = 1112.35 \text{ A}$$

$$i_{sq} = \sqrt{\frac{2}{3}} \operatorname{Im}[I_{s,dq}] = -1083.7 \text{ A}$$

As you can see i_{sd} & i_{sq} from the analytical solution matches the curves in figure 3 for the first part in the simulation.

$$V_m = V_s - I_s(R_s + j\omega_s L_{ls}) = 306.773 - j20.16 \text{ V}$$

$$I_m = \frac{V_m}{jX_m} = -35.05 - j533.25 \text{ A}$$

$$I_r = I_s - I_m = 680.03 - j89.6 \text{ A}$$

$$I_{r,dq} = \frac{-3\sqrt{2}}{2} I_r = -1442.556 + j190.072 \text{ A}$$

$$i_{rd} = \sqrt{\frac{2}{3}} \operatorname{Re}[I_{r,dq}] = -1177.84 \text{ A}$$

$$i_{rq} = \sqrt{\frac{2}{3}} \operatorname{Im}[I_{r,dq}] = 155.19 \text{ A}$$

Again also for i_{rd} & i_{rq} from the analytical calculation are almost the same as the curves in figure 3 for the first part of the simulation at $T = 5000 \text{ Nm}$. By applying the transformation matrices above for rotor and stator currents we get

By repeating the above calculation at $T = -5000 \text{ Nm}$ at slip $s = -6.87 \times 10^{-3}$ we get:

$$T_{em} = T_L = -5000$$

To reach a steady state speed without accelerating.

$$\omega_{mech} = \omega_s * (1 - s) = 126.53 \text{ rad/sec}$$

$$i_{sd} = -1072.79 \text{ A}$$

$$i_{sq} = -1110.6 \text{ A}$$

$$i_{rd} = 1148.25 \text{ A}$$

$$i_{rq} = 171.44 \text{ A}$$

By using the transformation matrix below for rotor and stator currents in dq reference frame we get the currents in abc reference frame as in figures 4 & 5 where they almost have very close frequencies since the slip is small.

$$\begin{bmatrix} i_a(t) \\ i_b(t) \\ i_c(t) \end{bmatrix} = \sqrt{\frac{2}{3}} \begin{bmatrix} \cos(\theta_{da}) & -\sin(\theta_{da}) \\ \cos(\theta_{da} + \frac{4\pi}{3}) & -\sin(\theta_{da} + \frac{4\pi}{3}) \\ \cos(\theta_{da} + \frac{2\pi}{3}) & -\sin(\theta_{da} + \frac{2\pi}{3}) \end{bmatrix} \begin{bmatrix} i_{sd}(t) \\ i_{sq}(t) \end{bmatrix}$$

$$\begin{bmatrix} i_A(t) \\ i_B(t) \\ i_C(t) \end{bmatrix} = \sqrt{\frac{2}{3}} \begin{bmatrix} \cos(\theta_{dA}) & -\sin(\theta_{dA}) \\ \cos(\theta_{dA} + \frac{4\pi}{3}) & -\sin(\theta_{dA} + \frac{4\pi}{3}) \\ \cos(\theta_{dA} + \frac{2\pi}{3}) & -\sin(\theta_{dA} + \frac{2\pi}{3}) \end{bmatrix} \begin{bmatrix} i_{rd}(t) \\ i_{rq}(t) \end{bmatrix}$$

Part B

In this part, the rotor side converter (RSC) is modelled as a simple voltage gain of $\frac{V_{DC}}{2}$. The turbine model is added to the model in part A based and the grid side orientation and rotor side converter controller are added as well. The turbine model is added based on the below equations which are the equations recommended by the supplier.

$$P_{mech} = \frac{1}{2} \rho A_r V_w^3 C_p(\lambda, \theta)$$

Where,

λ : Tip speed ratio

θ : Pitch angle (kept at zero to capture maximum power)

V_w : Wind Velocity

$$\frac{1}{2} \rho A_r = 2311$$

$$C_p(\lambda, \theta) = c_1 \left(\frac{c_2}{\lambda_i} - c_3 \theta - c_4 \right) e^{-\frac{c_5}{\lambda_i}}$$

$$\frac{1}{\lambda_i} = \frac{1}{\lambda + 0.08\theta} - \frac{0.035}{\theta^3 + 1}$$

$$\lambda = K_b \left(\frac{\omega_{mech}}{V_w} \right)$$

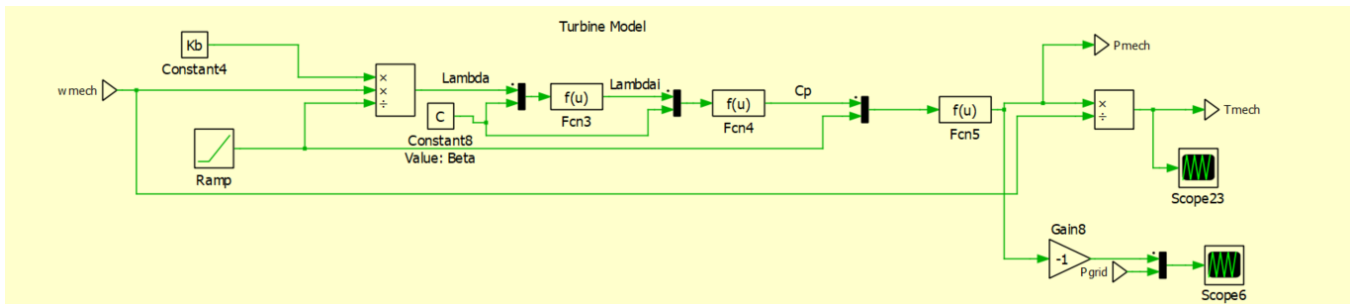


Figure 7 Turbine model in PLECS

The above model in PLECS is added to the model in part A. Then rotor side converter controllers are added as well. The speed control loop gives the torque reference required which is used to generate the rotor current reference in d frame based on the below equation

$$i^*_{rd} = -\frac{2}{P} \omega_s \frac{L_s}{L_m} \frac{1}{v_{sd}} T^*_{em}$$

When designing the speed controller the torque loop is assumed to be ideal since the torque loop has high bandwidth compared to the speed loop. The controller is designed using type 2 K-factor controller

method with required phase margin of 60 degrees and at controller bandwidth of 100 hz using the below transfer function.

$$\frac{\omega_{mech}(S)}{T_{em}(S)} = \frac{1}{SJ_{eq} + B}$$

Where,

J_{eq} : Moment of inertia of the system

B : Coeffecient of friction

The speed loop is shown in figure 8, the supplementary grid support control is not discussed in this document. Reactive power can also be controller based on the below equation where it is obvious that it will be controlled by controlling i_{rq} as the rest of the equation are constants.

$$Q_s = \frac{(v_{sd})^2}{\omega_s L_s} + \frac{L_m}{L_s} v_{sd} i_{rq}$$

The objective of this part is to have unity power factor which means that the reactive power shall be equal to 0.

Then,

$$i^{*}_{rq} = -\frac{v_{sd}}{\omega_s L_m}$$

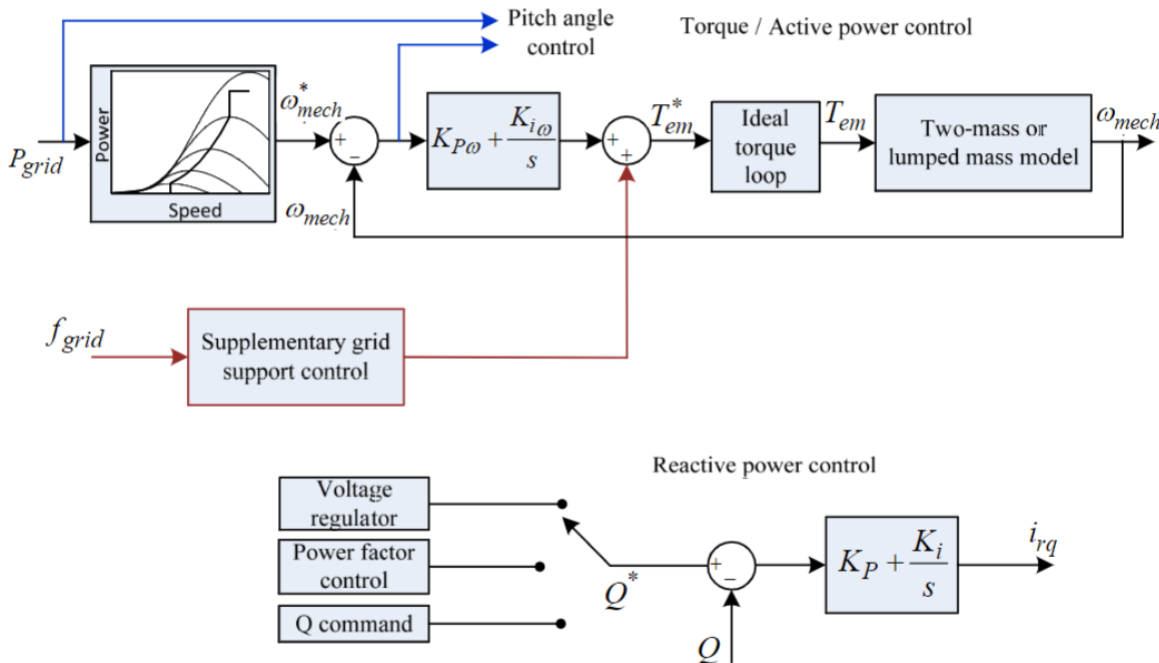


Figure 8 Active and Reactive power control block diagram

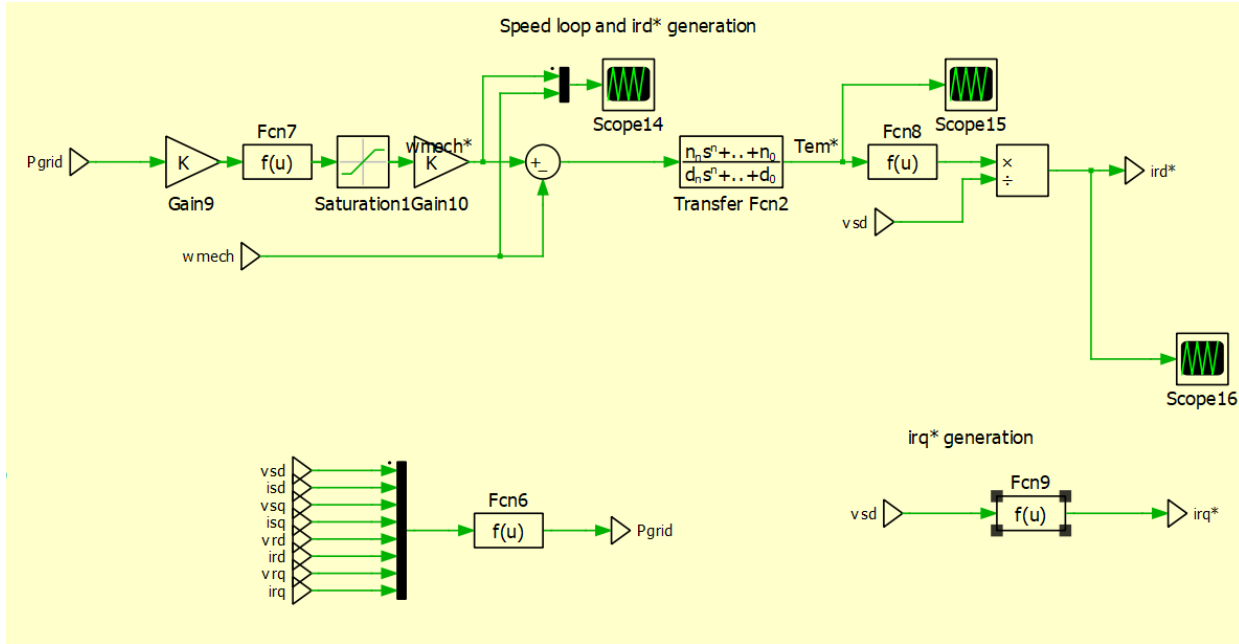


Figure 9 Active and reactive power control in PLECS

The currents generated from the power and reactive power control loops are then fed to the current control loops which are modeled based on the below equations.

$$v_{rd} = \left(R_r i_{rd} + \sigma L_r \frac{di_{rd}}{dt} \right) - \omega_{dA} \sigma L_r i_{rq}$$

$$v_{rq} = \left(R_r i_{rq} + \sigma L_r \frac{di_{rq}}{dt} \right) + \omega_{dA} \sigma L_r i_{rd}$$

Where the cross-coupling terms in the two equations are cancelled by adding feedforward as shown in figure 10, leading to the below transfer functions which are used to control rotor side currents.

$$\frac{i_{rd}(S)}{v_{rd\ c}(S)} = \frac{V_{DC}/2}{R_r + S\sigma L_r}$$

$$\frac{i_{rq}(S)}{v_{rq\ c}(S)} = \frac{V_{DC}/2}{R_r + S\sigma L_r}$$

Where $v_{rd\ c}$ and $v_{rq\ c}$ are the dq axis controller outputs and the inverter is modelled as simple gain.

The two transfer functions are identical which mean they will have the same controller parameters. The controller is also designed using type 2 K-factor controller. The required phase margin is 60 degrees and the controller bandwidth is 10 Khz which is much higher than the speed loop.

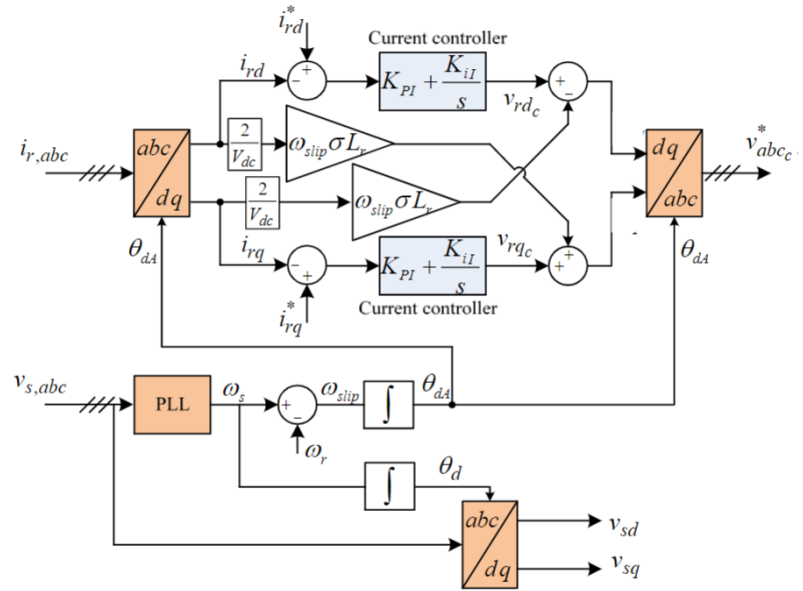


Figure 10 Rotor current control block diagram

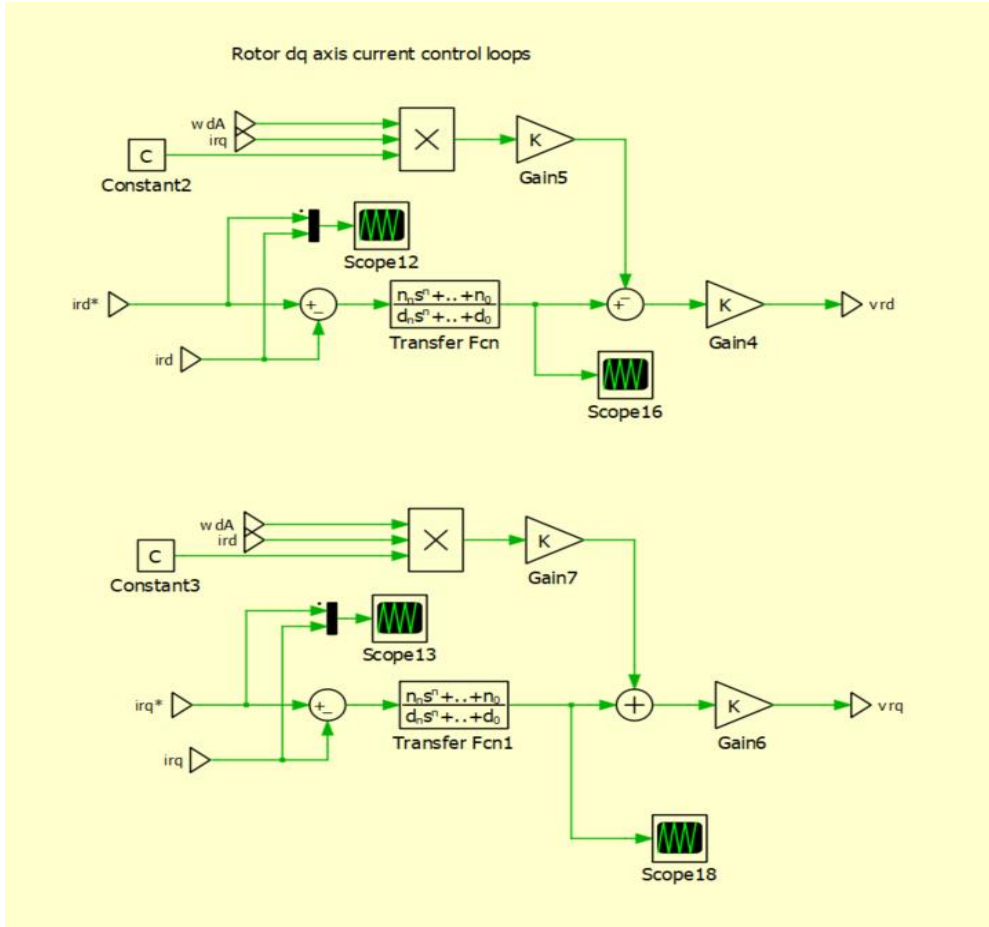


Figure 11 Rotor current control PLECS model

The model is analyzed at two different wind speeds, 8 and 12 m/sec and compared to calculated values analytically. Figure 12 shows the mechanical speed of the rotor for both wind speeds. It is noticed that in case of 12 m/sec wind speed, the mechanical speed is much higher and this is due to the higher torque provided to the generator through MPPT which increases the power extracted and hence the higher the speed due to the equation provided by the supplier below.

$$\omega_{mech,ref} = -0.67P^2 + 1.42P + 0.51$$

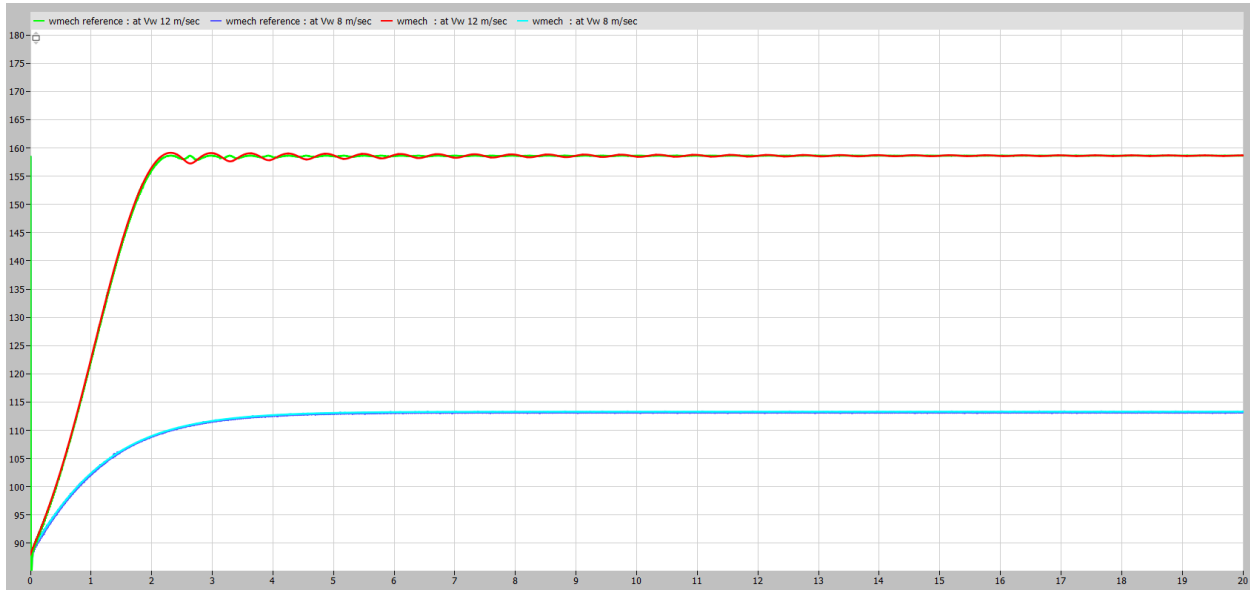


Figure 12 Mechanical speeds at for wind speeds

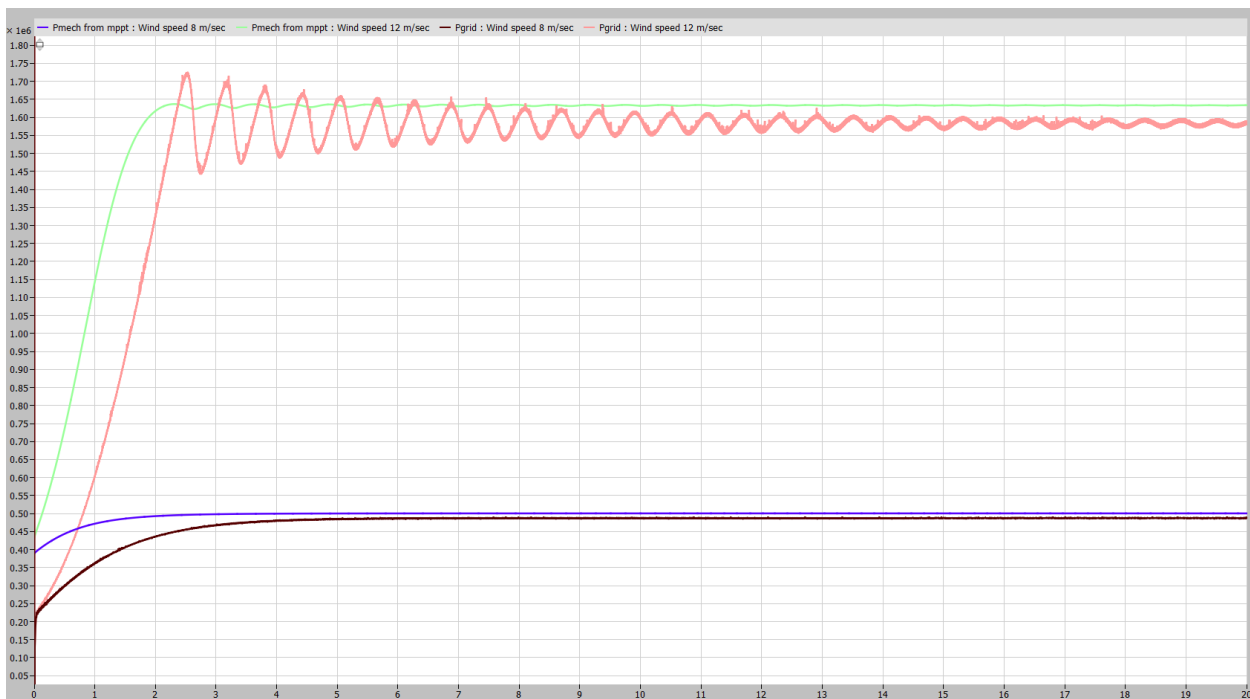


Figure 13 Mechanical Power from MPPT and grid injected power for different wind speeds

Figure 13 represents the mechanical power from MPPT and the power injected to the grid at the 2 wind speeds. Again, it is noticed that the power in case of the higher wind speed is higher than the power at low wind speed, which is expected. Also note that for each wind speed the mechanical power and grid injected power are not equal and the mechanical power is a bit higher which is reasonable since not all the power extracted from the wind will be injected to the grid as there are some losses in the system which represents this small difference.

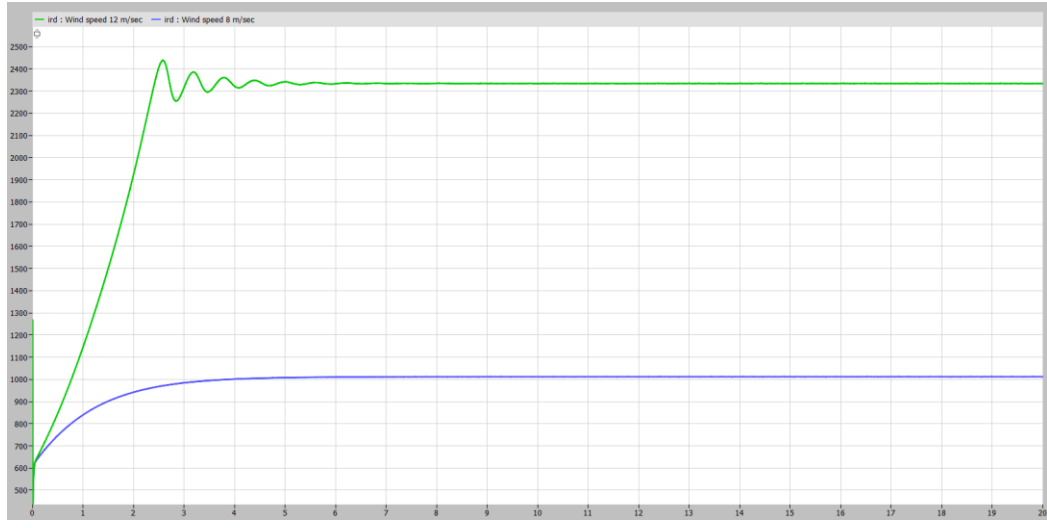


Figure 14 rotor d-axis current for different wind speeds

Figure 14 shows the rotor current of the d-axis. Since the rotor d-axis current is responsible for controlling the power or the torque, the higher the power the higher the current and this is shown in figure 14 where the current in the case of high wind speed is higher than that of the low wind speed.

Figure 15 shows the rotor q-axis currents for both wind speeds and they are identical for both cases as the q-axis rotor current is controlling the power factor by maintaining unity power factor so its main goal is to eliminate the effect of the stator q-axis current to have unity power factor. For both cases they have the same requirement for the power factor so they are identical.



Figure 15 rotor q-axis current for different wind speeds

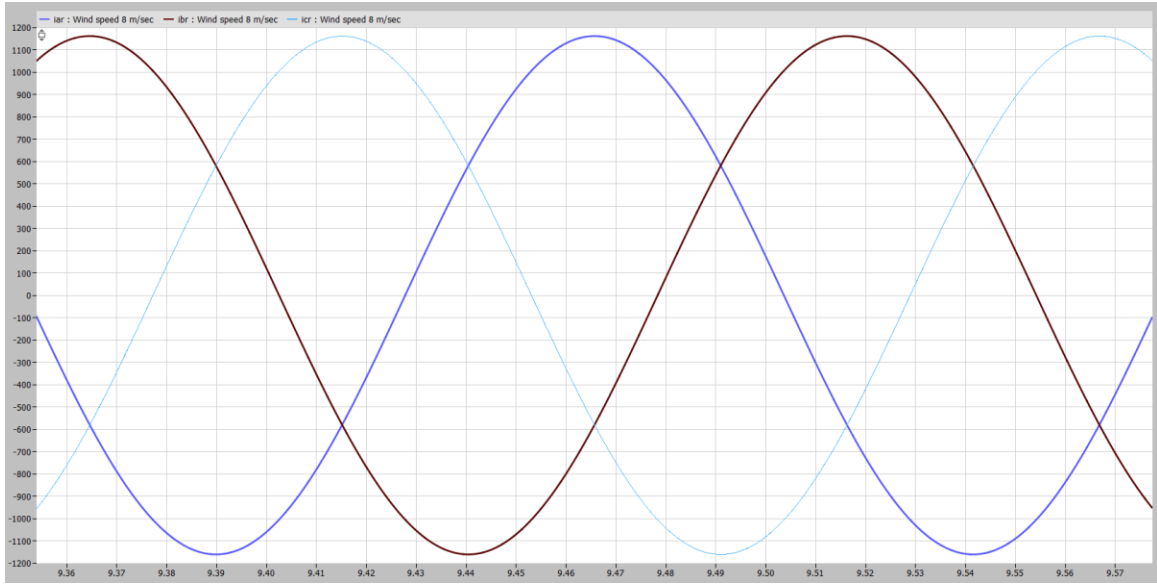


Figure 16 abc rotor current for wind speed 12 m/sec



Figure 17 abc rotor current for wind speed 12 m/sec

Figure 16 and 17 show the rotor currents in abc reference frame and it is as expected, the peak value in the case of high wind speed is larger than that of the low wind speed. For both cases, the currents have the frequency of ω_{dA} , which changes by changing the speed of the motor hence they have different frequencies.

Figure 18 represents the stator q-axis current which is mostly due to the magnetization current and they are almost the same for both cases. The small difference is due to the voltage drop in the stator resistance for both cases however it is very small and that is the reason why for both cases the rotor q-axis current is the same as well.

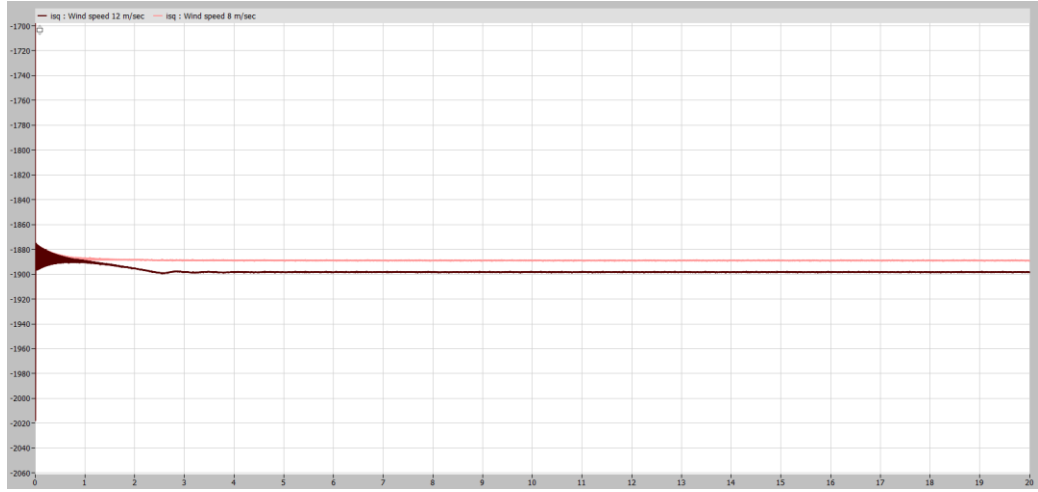


Figure 18 stator *q*-axis current for different wind speeds

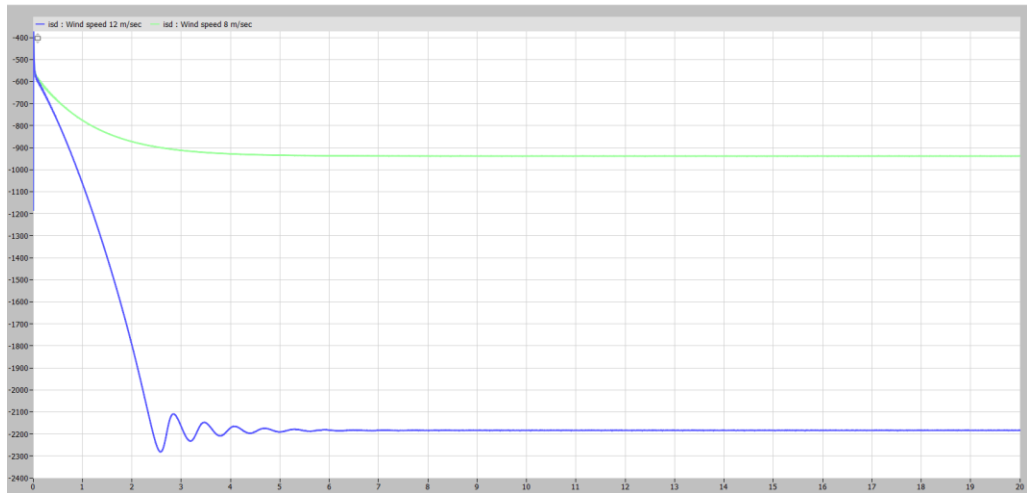


Figure 19 stator *d*-axis current for different wind speeds

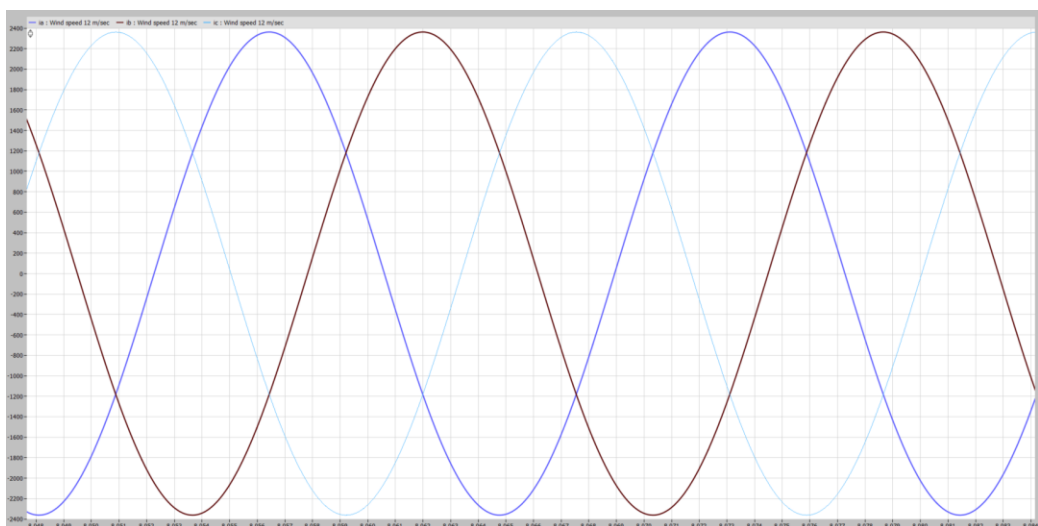


Figure 20 Stator *abc* current at wind speed 12 m/sec

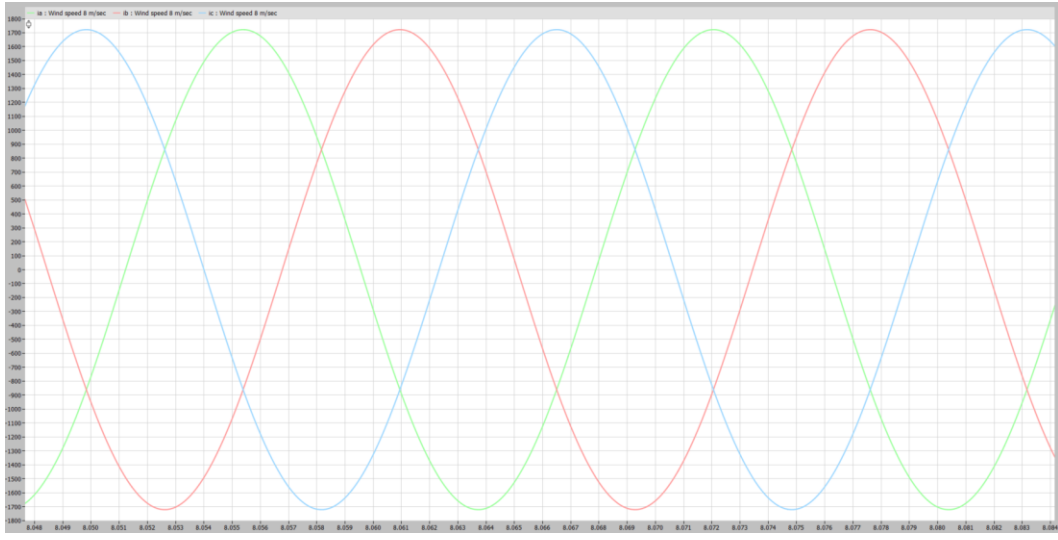


Figure 21 stator abc current at wind speed 8 m/sec

Figure 20 and 21 show the stator currents in abc reference frame and it is noticed that the amplitudes are different for both cases which is expected due to higher power and higher current however the frequency is the same which is the grid frequency 60 hz.

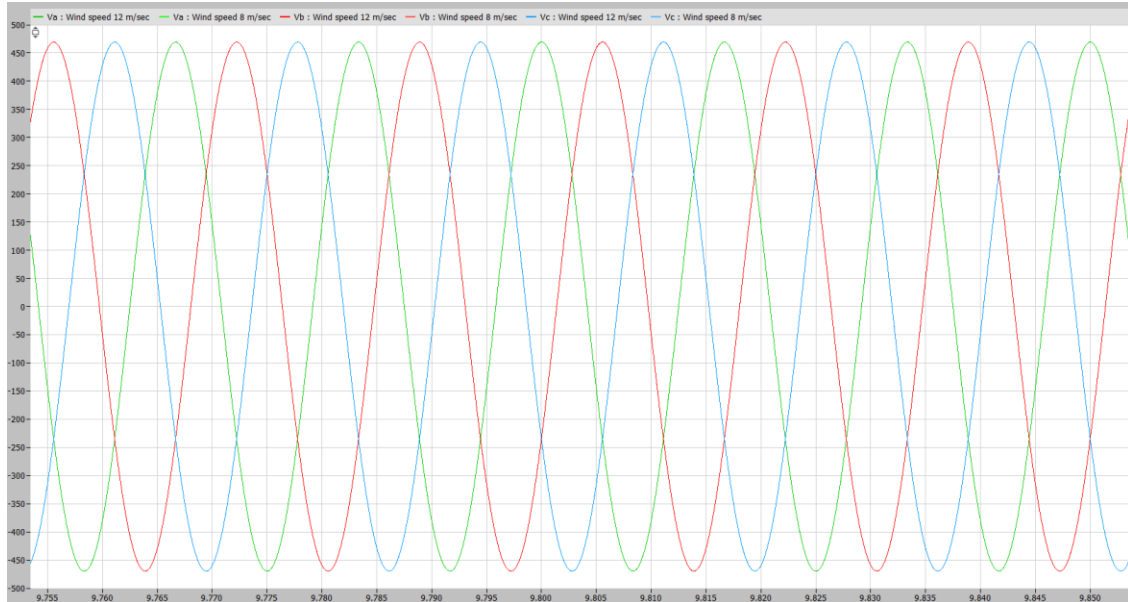


Figure 22 Stator abc voltages for different wind speeds

As seen in figure 22 abc voltages are always the same and independent of anything since they are related to the grid so they have the frequency and voltages of the grid. The same for the stator dq voltages, they are always the same where the voltage in q-axis is zero and the voltage in d-axis is the rms value of the line-to-line voltage of the grid as shown in figure 23.

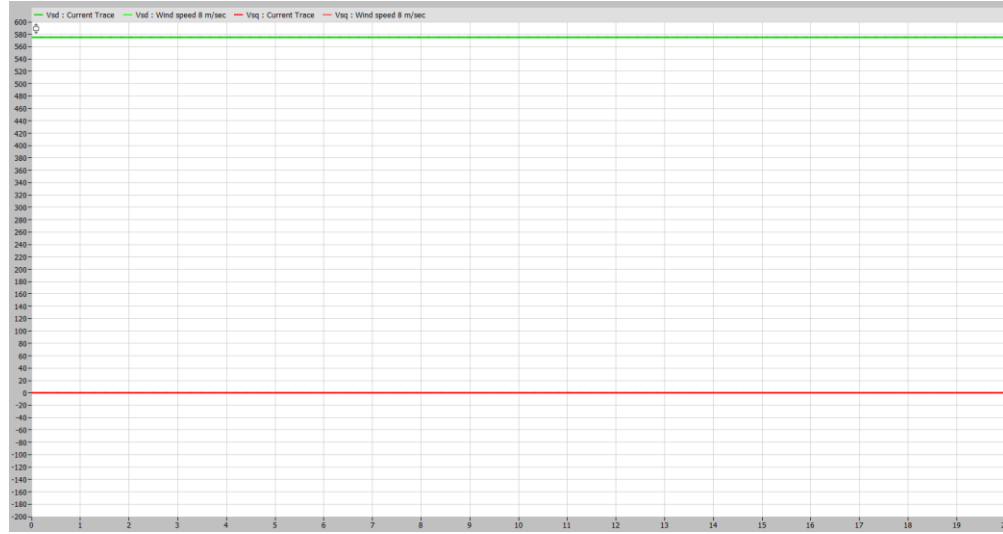


Figure 23 Stator dq voltages for different wind speeds

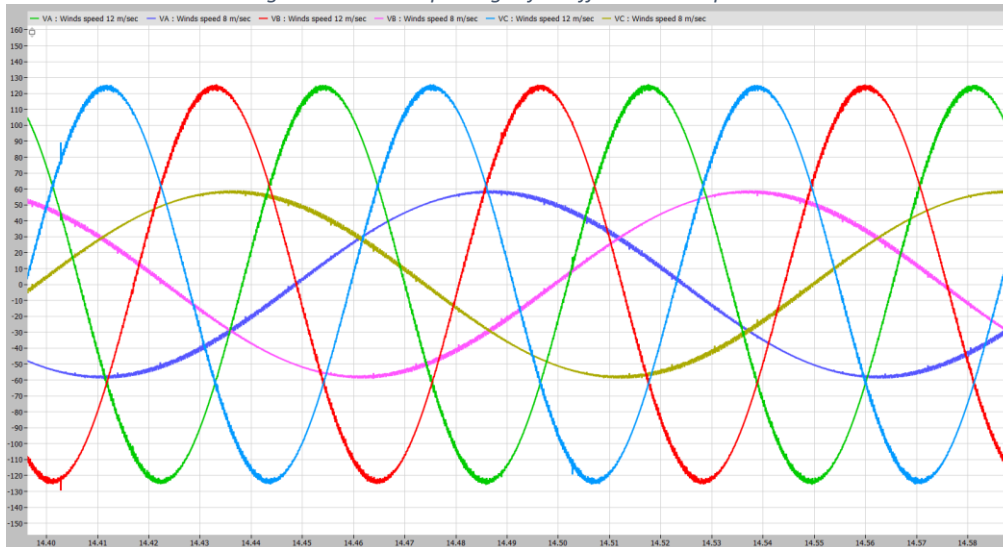


Figure 24 Rotor abc voltages for different wind speeds

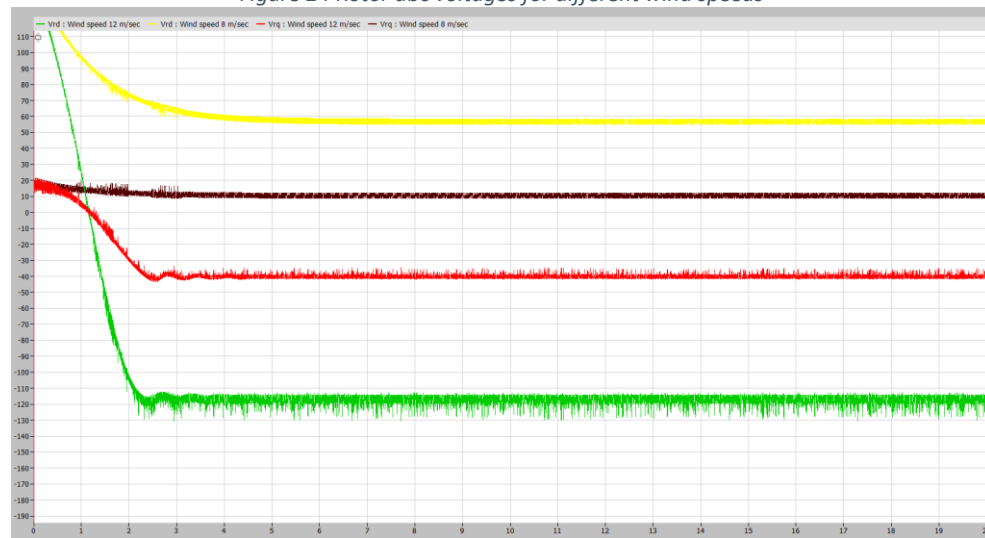


Figure 25 Rotor dq voltages for different wind speeds

Figure 24 shows the change of amplitude and frequency of the rotor voltages by changing the wind speed and the change of frequency is due to the change of rotor speed for both cases.

By solving this analytically, we get: For 8 m/sec wind speed (reference values are used for calculations assuming the controllers designed are robust and follow the reference values)

$$P_{mech} = \frac{1}{2} \rho A_r V_w^3 C_p(\lambda, \theta)$$

$$P_{mech} = 500.509 \text{ KW}$$

Which is the same as in figure 13. Assuming the efficiency is around 0.95 we get

$$P_{grid} = P_{mech} * 0.95 = 475.484 \text{ KW}$$

$$\omega_{mech,ref} = -0.67P^2 + 1.42P + 0.51$$

$$\omega_{mech,ref} = 114.26 \text{ rad/sec}$$

Noting that:

$$P_{base} = 1.5 \text{ MW} \quad \omega_{base} = \omega_{synch} = 125.66 \text{ rad/sec}$$

The speed calculated is almost the same as in figure 12.

$$i_{rq} = -\frac{v_{sd}}{\omega_s L_m}$$

$$i_{rq} = 999.5A$$

$$i_{rd} = -\frac{2}{P} \omega_s \frac{L_s}{L_m} \frac{1}{v_{sd}} T^*_{em}$$

$$i_{rd} = 1016.74A$$

Rotor currents are the same in figures 14 and 15.

$$v_{rd} = \left(R_r i_{rd} + \sigma L_r \frac{di_{rd}}{dt} \right) - \omega_{dA} \sigma L_r i_{rq}$$

$$v_{rd} = 56V$$

$$v_{rq} = \left(R_r i_{rq} + \sigma L_r \frac{di_{rq}}{dt} \right) + \omega_{dA} \sigma L_r i_{rd}$$

$$v_{rq} = 9.4V$$

Rotor voltages are the same as in figure 25.

Stator voltages are the grid voltage so it the same and the dq is just the transformation at 60 hz frequency which makes q voltage = 0 and d voltage = Line-to-line rms voltage of the grid.

To get the currents or voltages in abc from dq frame you can use the below transformation.

$$\begin{bmatrix} i_a(t) \\ i_b(t) \\ i_c(t) \end{bmatrix} = \sqrt{\frac{2}{3}} \begin{bmatrix} \cos(\theta_{da}) & -\sin(\theta_{da}) \\ \cos(\theta_{da} + \frac{4\pi}{3}) & -\sin(\theta_{da} + \frac{4\pi}{3}) \\ \cos(\theta_{da} + \frac{2\pi}{3}) & -\sin(\theta_{da} + \frac{2\pi}{3}) \end{bmatrix} \begin{bmatrix} i_{sd}(t) \\ i_{sq}(t) \end{bmatrix}$$

$$\begin{bmatrix} i_A(t) \\ i_B(t) \\ i_C(t) \end{bmatrix} = \sqrt{\frac{2}{3}} \begin{bmatrix} \cos(\theta_{dA}) & -\sin(\theta_{dA}) \\ \cos(\theta_{dA} + \frac{4\pi}{3}) & -\sin(\theta_{dA} + \frac{4\pi}{3}) \\ \cos(\theta_{dA} + \frac{2\pi}{3}) & -\sin(\theta_{dA} + \frac{2\pi}{3}) \end{bmatrix} \begin{bmatrix} i_{rd}(t) \\ i_{rq}(t) \end{bmatrix}$$

For the rest of this part, the same model is tested by changing the wind speed to study the system dynamics and the robustness of the controllers. The wind velocity changes from 6m/sec to 12m/sec by ramp of slope 1m/sec. The following figures represent the results of the model test.



Figure 26 Mechanical speed reference and measured

Figure 26 shows the change in the speed of the rotor due to change of the wind because the MPPT changes the speed reference value. As it shown the measured speed follows the reference speed by the K-factor controller.

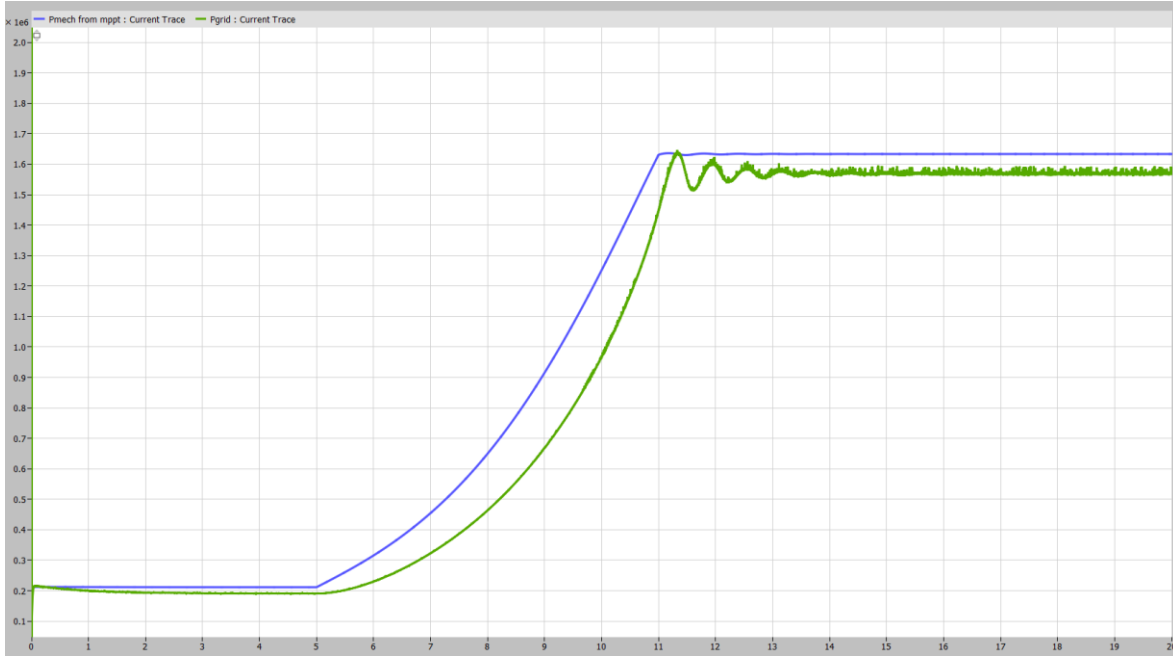


Figure 27 Mechanical power and power grid injected power

Figure 27 shows the change of the power extracted from the wind as well as the power injected to the grid by changing the wind speed. The difference between both powers represent the losses in the system.

Stator voltages are the same as in figures 22 and 23 as the grid voltage and frequency are the same.

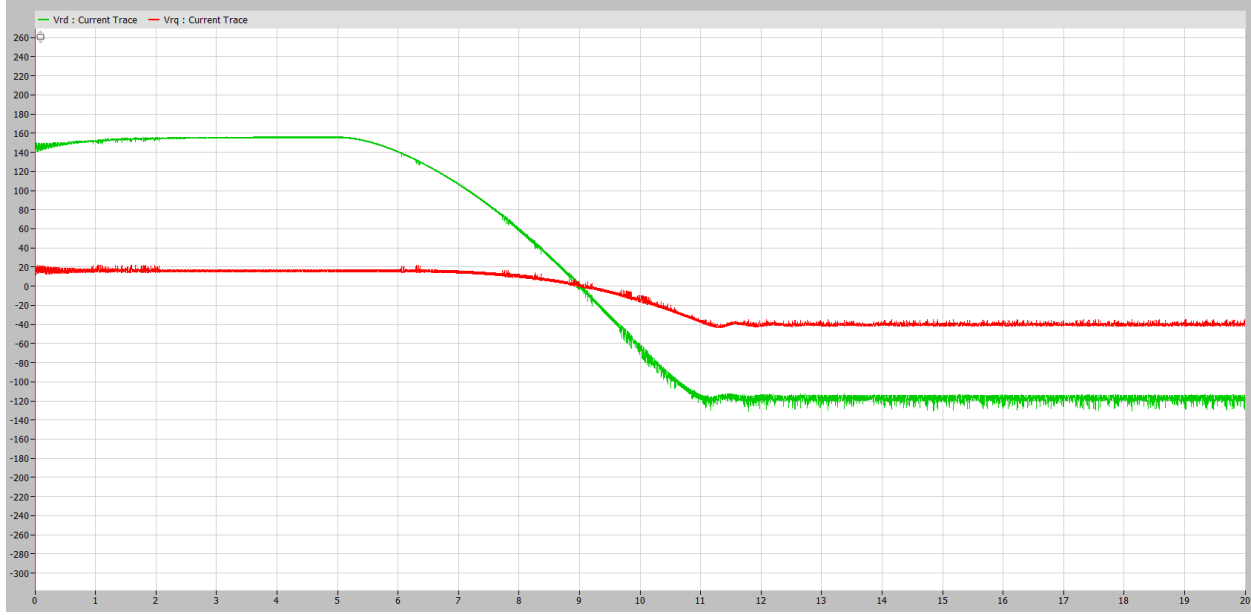


Figure 28 Rotor dq-axis voltages

Figure 28 shows the change in dq-axis voltages and from this figure we can notice the change from sub-synchronous to super-synchronous modes of operation when the rotor d-axis voltage changes from positive to negative.

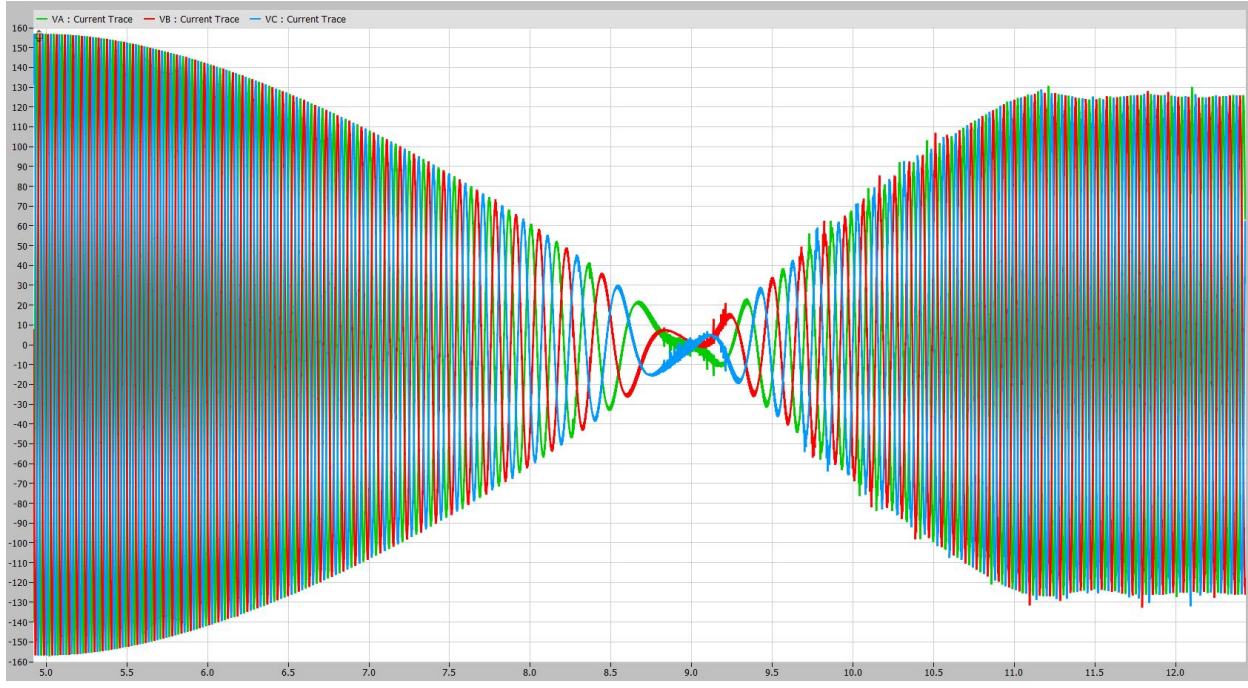


Figure 29 Rotor abc reference frame voltages

You can also notice the change in mode of operation in the abc reference frame and you can also notice the change in frequency of the waveform due to change of the rotor speed.

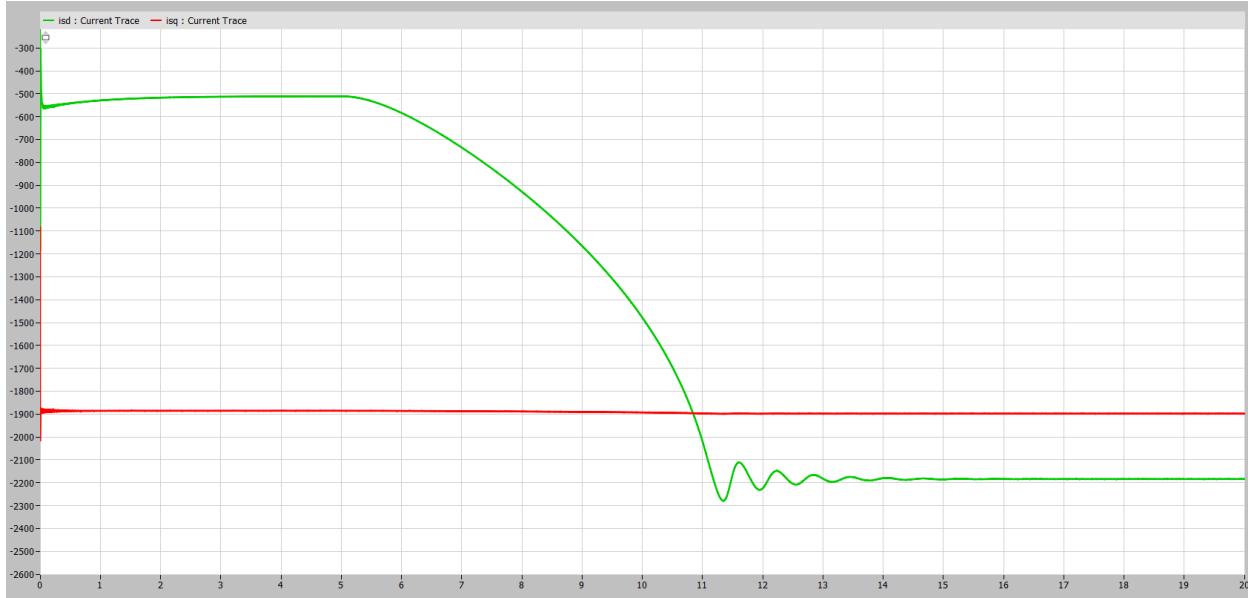


Figure 30 Rotor side dq-axis currents

As shown in figure 30, the q-axis stator current is almost the same in both cases as the magnetizing current is almost the same however, the d-axis current changes by changing the rotor speed as the power injected to the grid changes as well. In figure 31, it is noticed that the frequency of the currents are not changed and inherit the frequency of the grid.

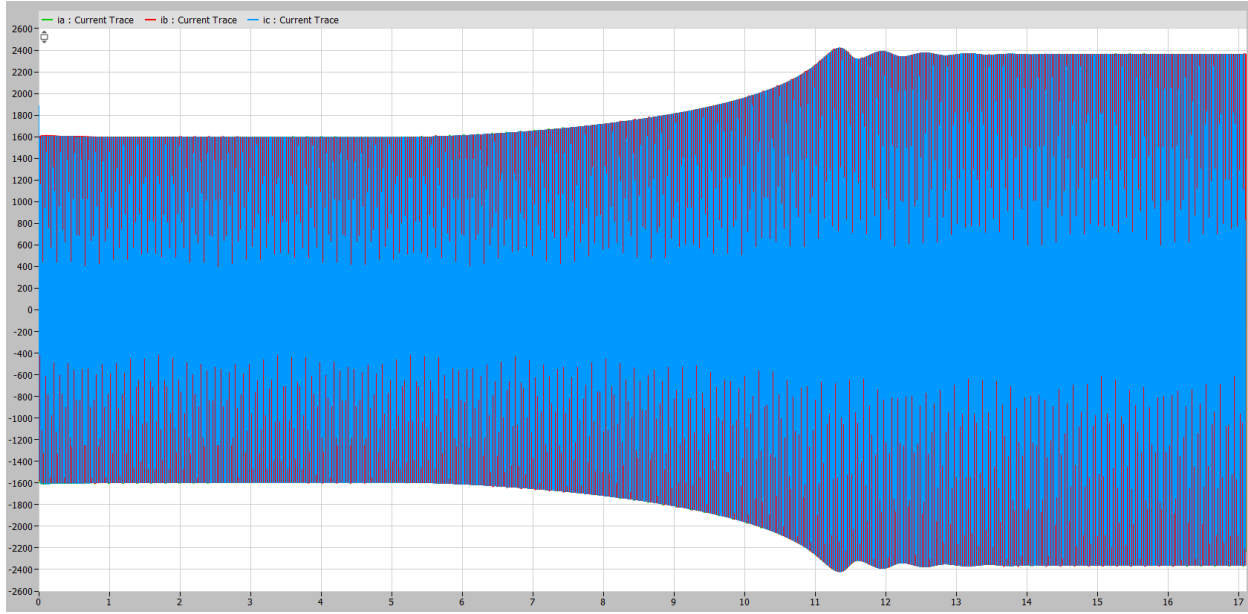


Figure 31 Stator abc reference frame currents

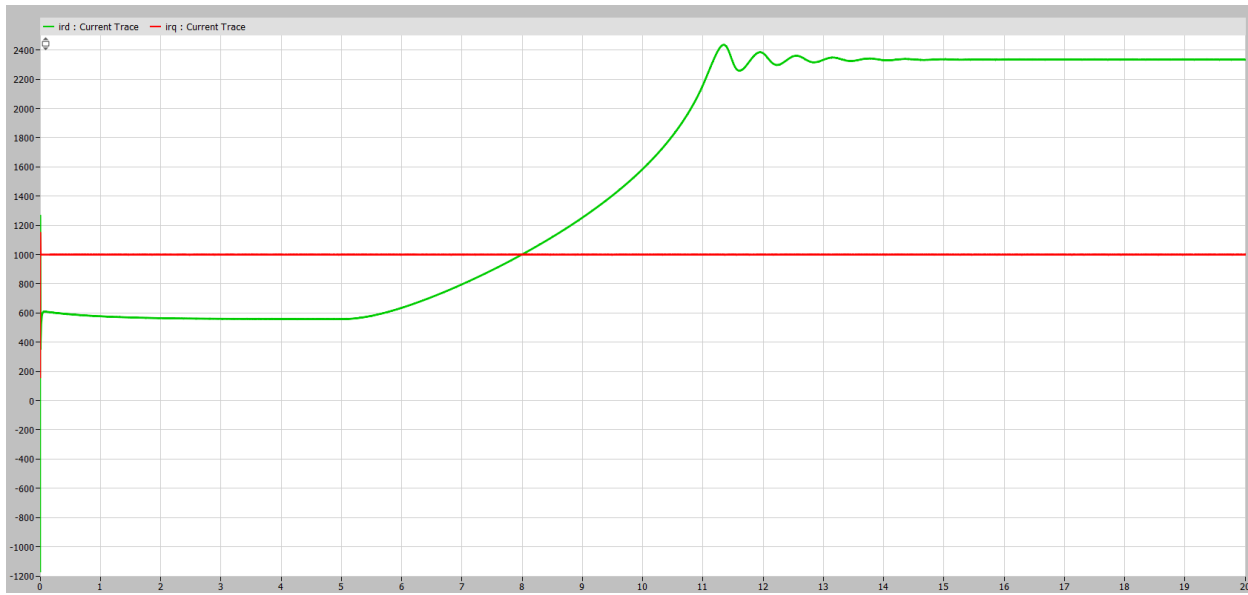


Figure 32 Rotor dq-axis currents

As expected, the q-axis current does not change as the q-axis stator current did not change or have slight change so the power factor is still maintained unity. Figure 32 also shows the change in the d-axis current that results from the change in motor speed.

Figure 33 shows the expected change in the current magnitudes in abc reference frame due to the change of the magnitude of d-axis current. The change in frequency of the current waveform shown in figure 33 is due to the change the frequency or the speed of the rotor.

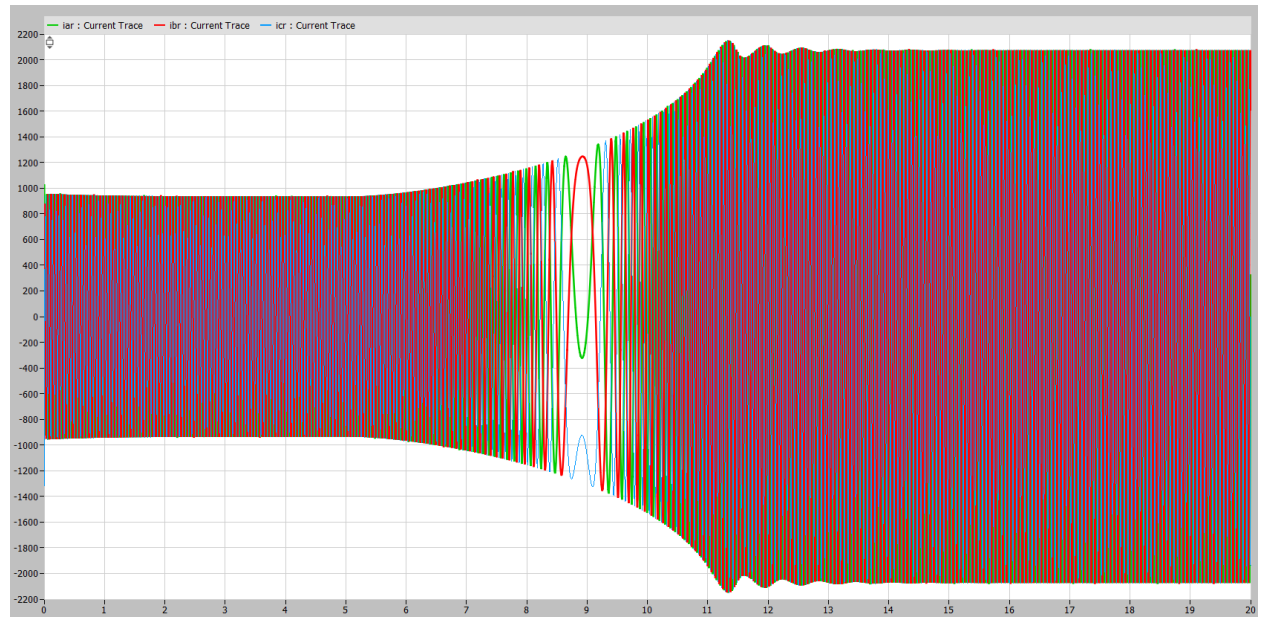


Figure 33 abc reference frame rotor currents

Part C

In this part both RSC and GSC are modeled and added to the model. Sinusoidal PWM is used at 10khz which introduces ripples in the system compared to part A and B as they were averaged models. The 2 converters are modeled as shown below in figure 34 and integrated with the rest of the model so that RSC now is not a simple gain but we use the circuit switched model. Dc link is not an ideal voltage source anymore, instead a real capacitor model is used.

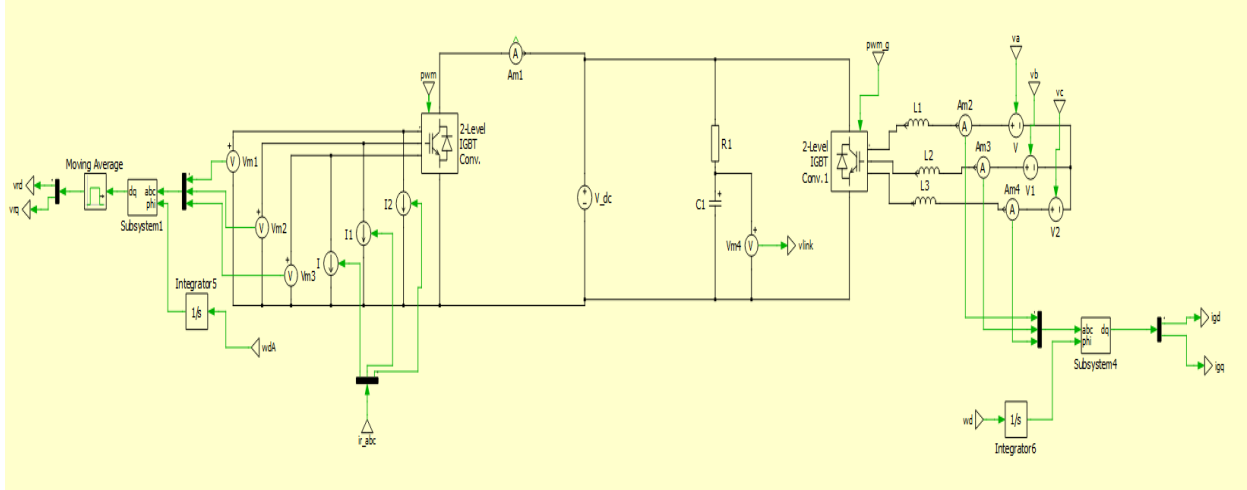


Figure 34 RSC and GSC models in PLECS

The GSC currents are being controlled such that the q-axis is used to control the reactive power and the d-axis current is used to control the DC link to maintain the bidirectional power flow between DC link and grid. The current control block diagram is as in figure 34.

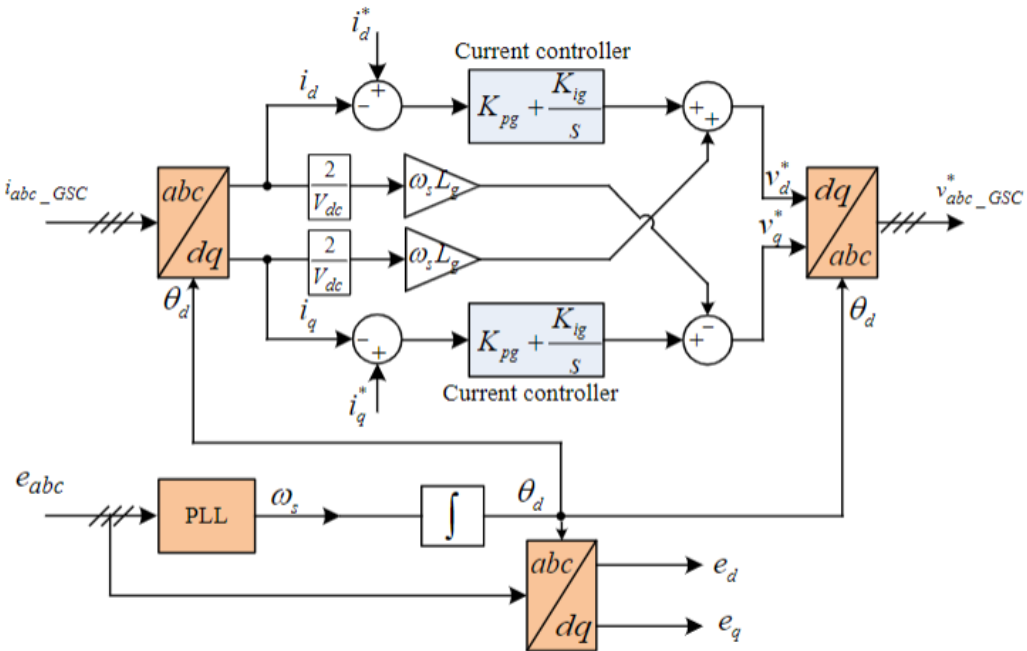


Figure 35 GSC Current control block diagram

The current controllers are designed using type 2 K-factor controller based on the following transfer function that they both have with phase margin of 60 degrees and 10khz bandwidth controller.

$$\frac{i_d(S)}{v_{d\ c}(S)} = \frac{-V_{DC}/2}{R_g + SL_g}$$

$$\frac{i_q(S)}{v_{q\ c}(S)} = \frac{-V_{DC}/2}{R_g + SL_g}$$

The current control reference set points are generated from the P and Q control loops where the active power is controlled by controlling the DC link voltage and to make the transfer function linear and easy to control, the DC link voltage squared is controlled as shown in figure 36. The controller designed is type 2 K-factor controller at 1khz controller bandwidth based on the below transfer function.

$$\frac{V_{dc}^2(S)}{P(S)} = \frac{2}{SC_{dc}}$$

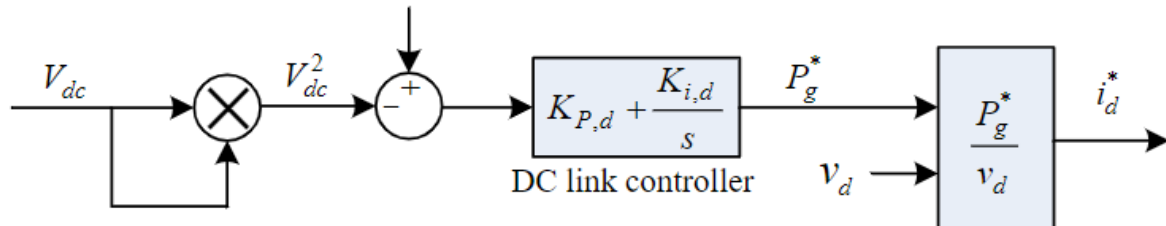


Figure 36 DC link voltage control block diagram

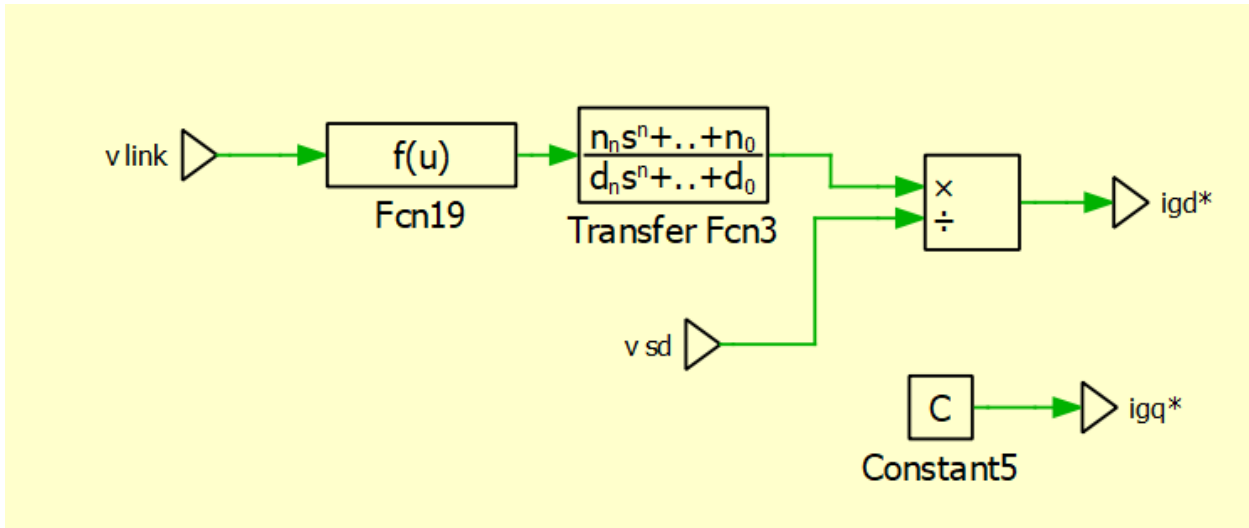


Figure 37 DC link voltage control in PLECS

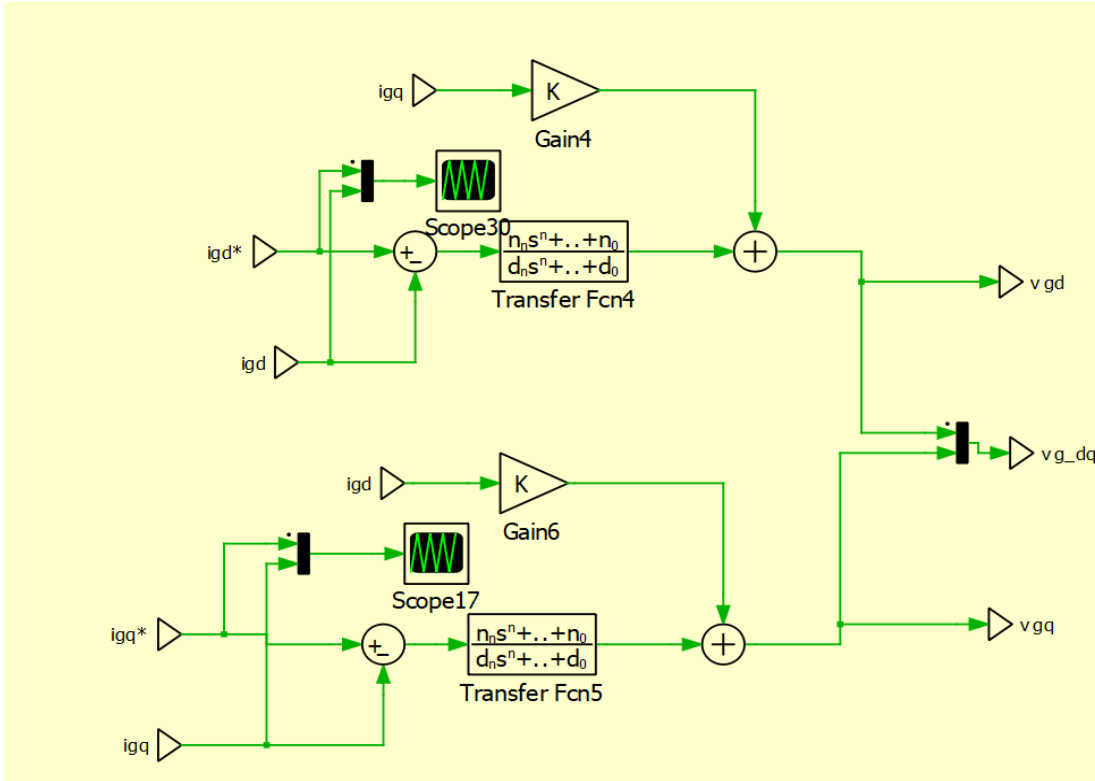


Figure 38 GSC current control in PLECS

The Q is controlled such that it is unity power factor. The overall system shown in figure 39 is analyzed at 2 different wind speeds 12 m/sec and 9 m/sec. The following figures show the performance and the analysis of the model.

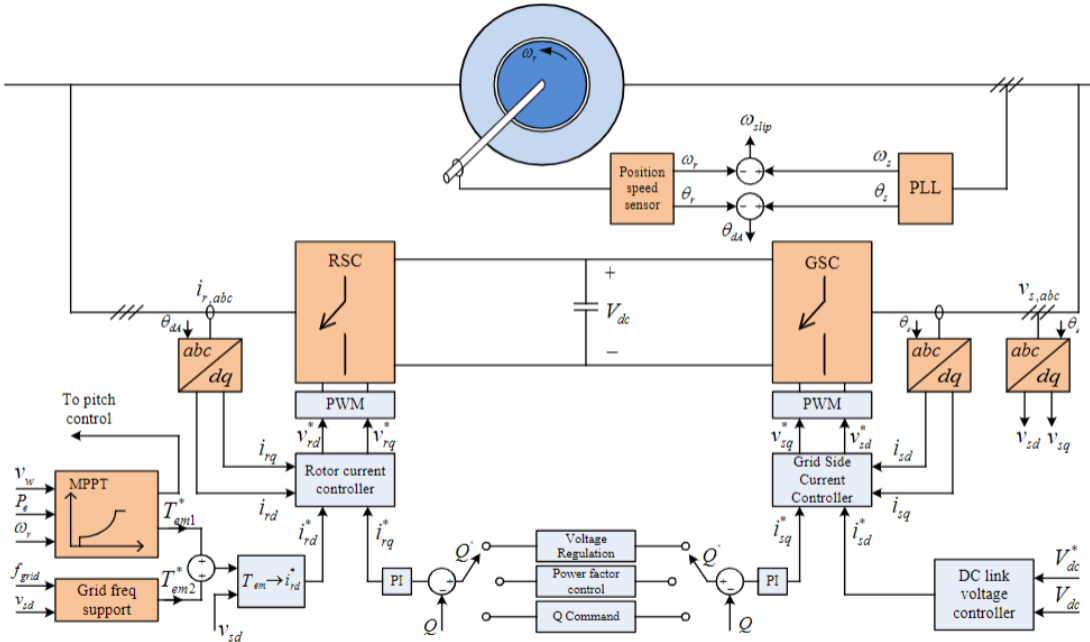


Figure 39 Over all block diagram of the system

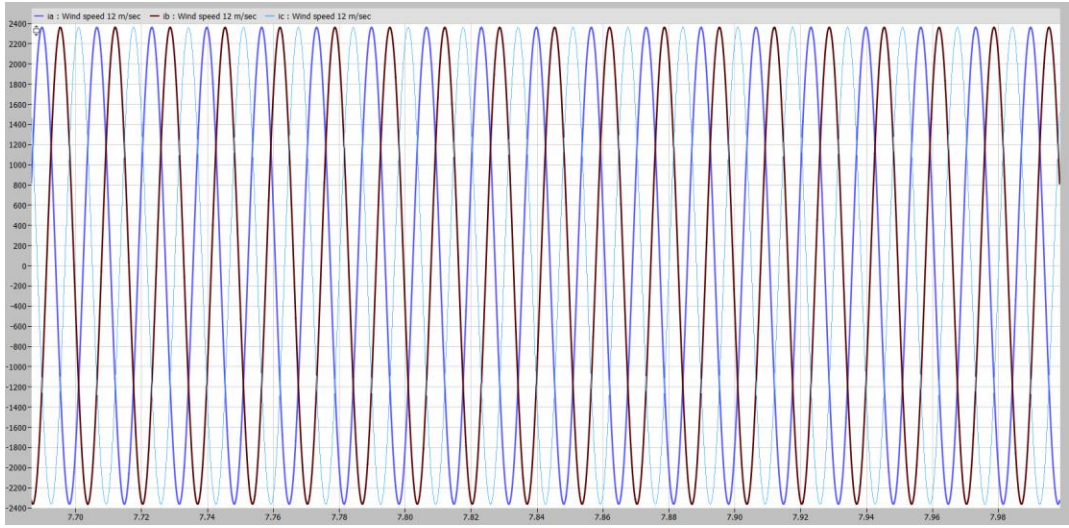


Figure 40 Stator abc current at wind speed 12 m/sec

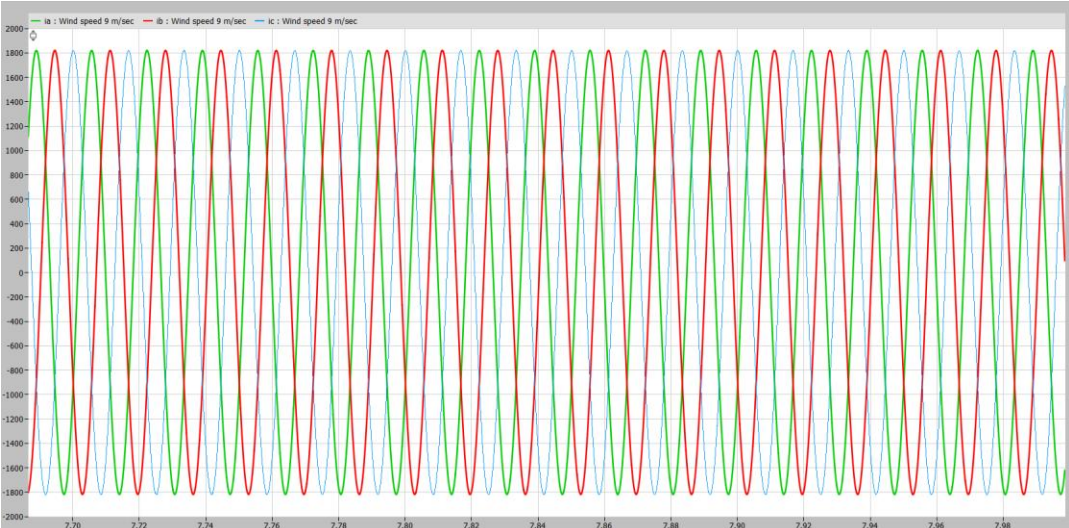


Figure 41 Stator abc current at wind speed 9 m/sec

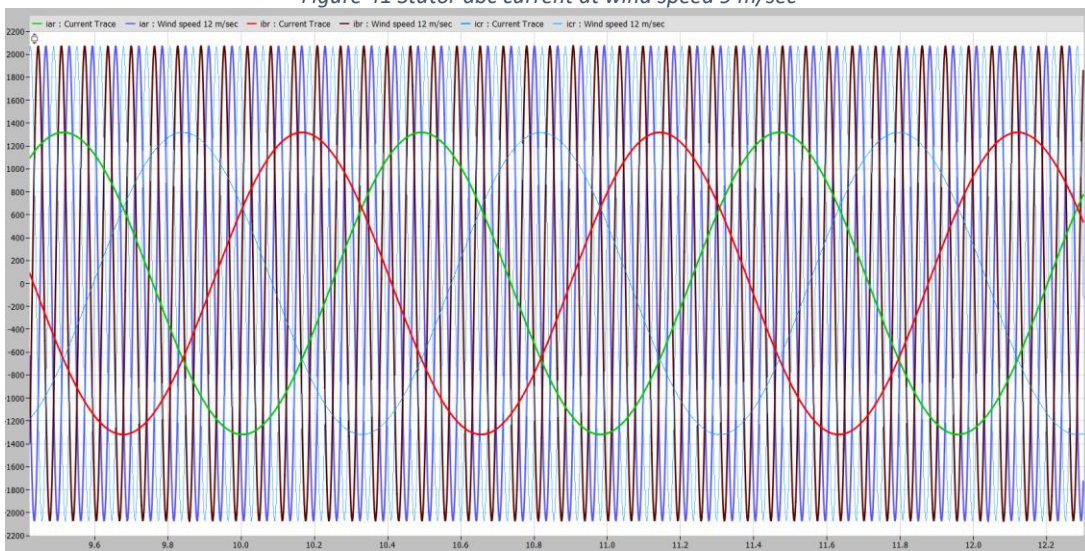


Figure 42 Rotor side abc currents at wind speeds 12 and 9 m/sec

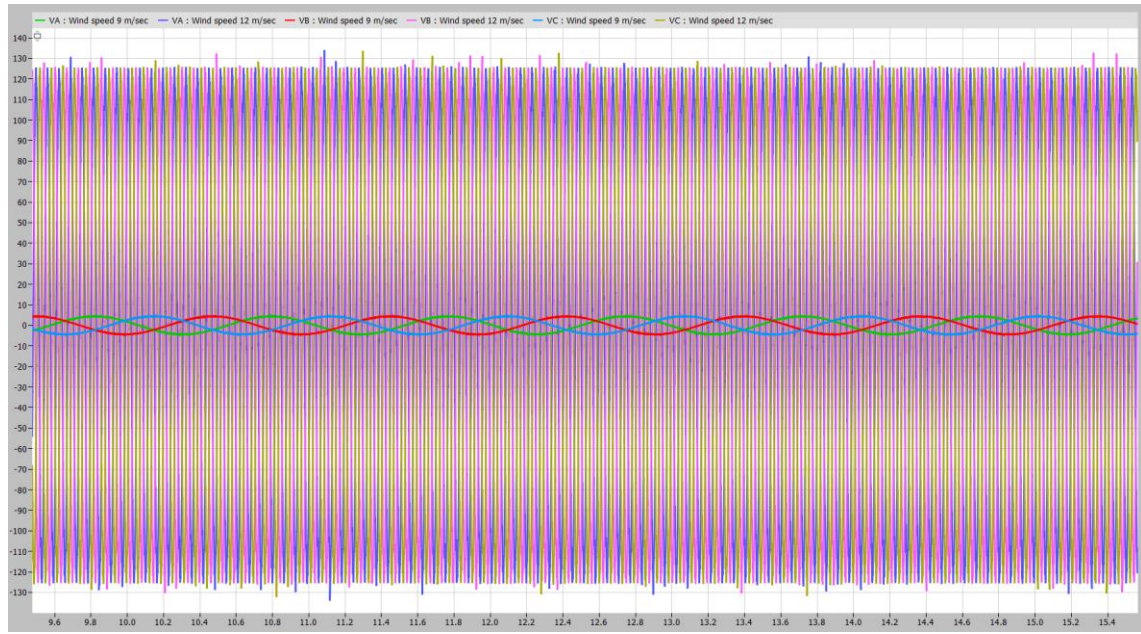


Figure 43 Rotor side abc voltages at wind speed 12 m/sec and 9 m/sec

As expected the currents and voltages of rotor and stator sides are almost the same as in part B however with the switching frequency ripple as this is not average model anymore.

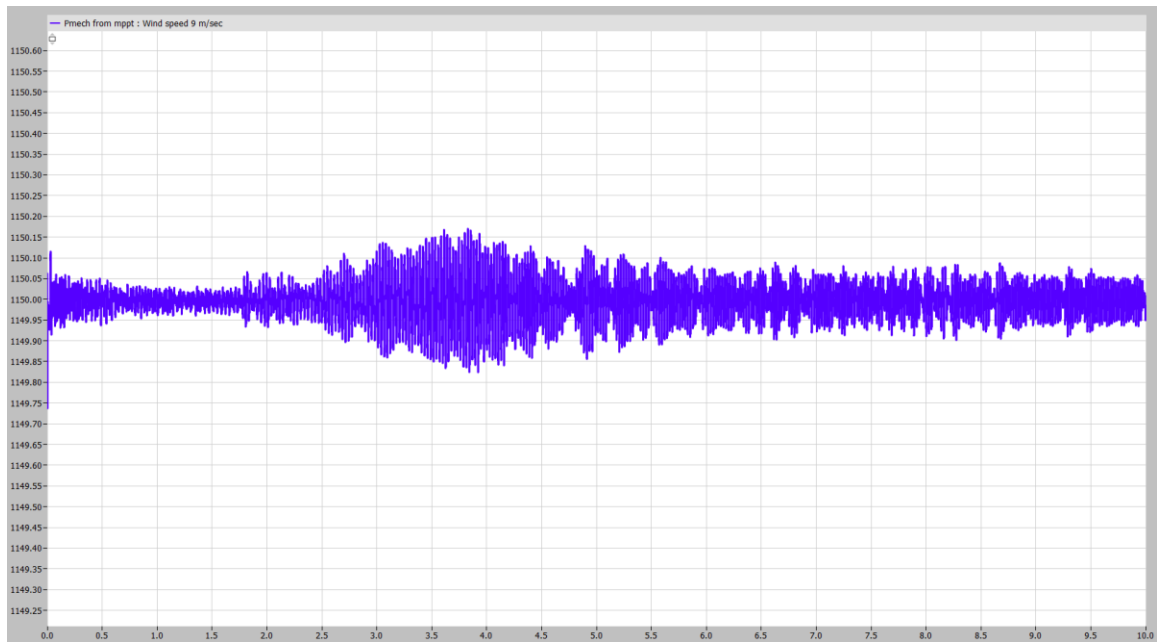


Figure 44 Vdc link at wind speed 9 m/sec

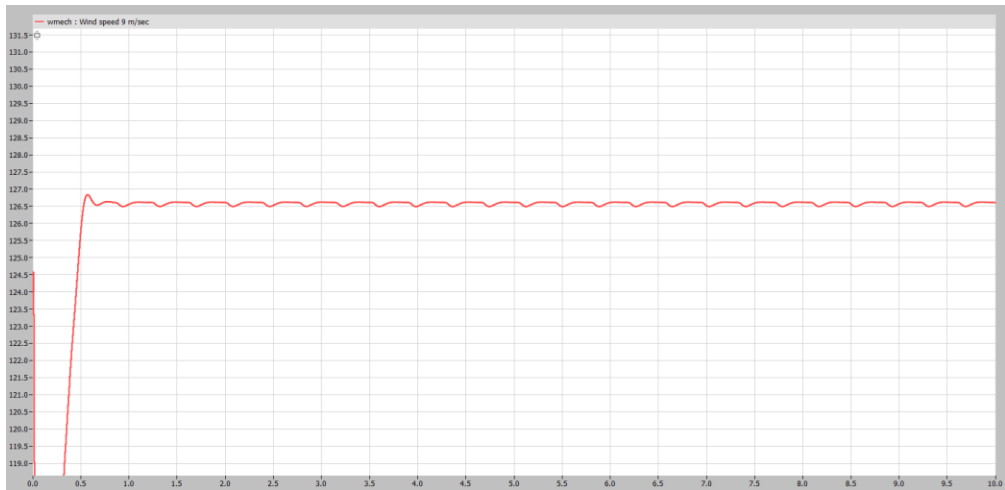


Figure 45 Rotor mechanical speed at wind speed 9 m/sec

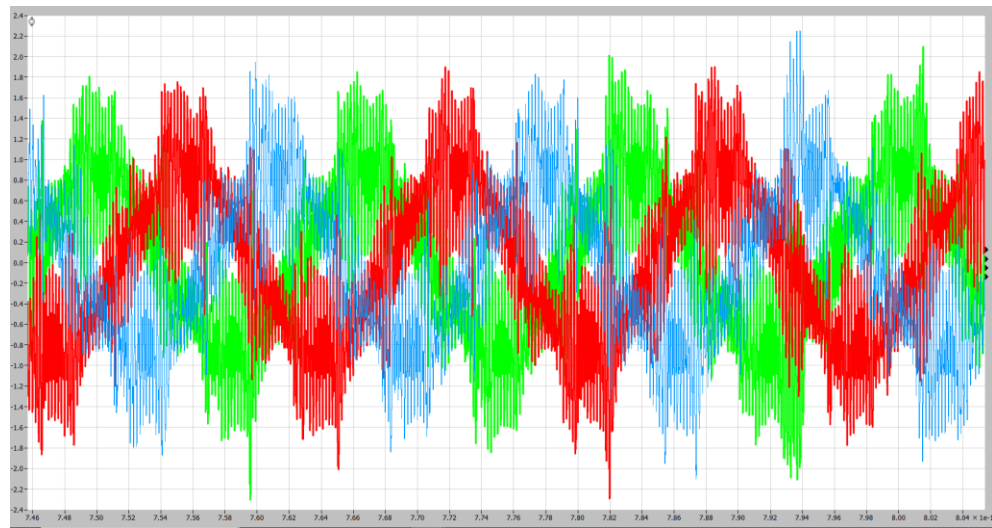


Figure 46 GSC voltage in abc axis at wind speed 9 m/sec

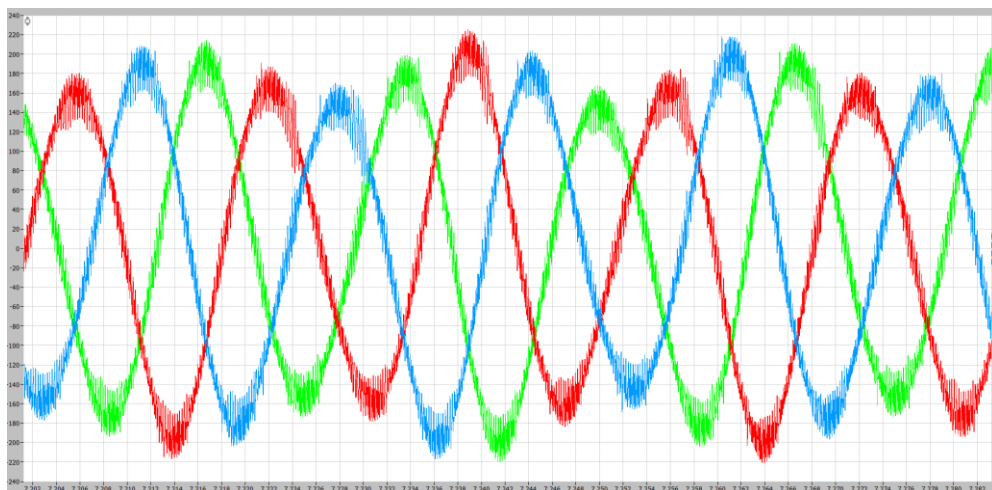


Figure 47 GSC current in abc frame at wind speed 9 m/sec

As expected all RSC values are the same as in part B but with ripples at the switching frequency.

Control design parameters

Speed controller	
ω_z	1684.5
ω_p	23436.28
K_c	1.058e4
RSC Current controllers	
ω_z	16847.5
ω_p	234362.81
K_c	317.23
GSC Current controllers	
ω_z	16845
ω_p	234362.81
K_c	-920.35
DC Link controller	
ω_z	1683.6
ω_p	92499.8
K_c	26445.93

Appendix

Appendix A

```
Lls = 0.0947e-3;
Llr = 0.0842e-3;
Lm = 1.526e-3;
Ls = Lm + Lls;
Lr = Lm + Llr;
M = [Ls 0 Lm 0; 0 Ls 0 Lm; Lm 0 Lr 0; 0 Lm 0 Lr];
M_inv = inv(M);
```